Towards Kilohertz Electrochemical Capacitors for Filtering and Pulse Energy Harvesting

Zhaoyang Fan[1,2*], Nazifah Islam[1,2], Stephen B. Bayne[1,3]

[1]Department of Electrical and Computer Engineering; [2]Nano Tech Center; [3]Center for Pulsed Power & Power Electronics; Texas Tech University, Lubbock, TX 79409-3102, United States.

*Email: Zhaoyang.Fan@ttu.edu

Keywords: High-frequency supercapacitor; kilohertz supercapacitor; electrochemical capacitor; electrolytic capacitor; nanostructured electrode; AC filtering

Abstract

Electrochemical capacitors (ECs) are slow devices with charging and discharging rates limited below 1 Hz. They run at direct current and function as power source, but cannot afford the role of a conventional capacitor for current ripple filtering or pulse energy harvesting. Recently, developing ultrafast ECs that work at hundreds to kilohertz (kHz) frequency scope have attracted great interests, with the aim to replace the traditional aluminum electrolytic capacitors (AECs) that have bulky size and large equivalent series resistance. Compact kHz ECs would produce huge impacts on power design, power electronics and environmental pulse energy harvesting. Towards such a goal, the electrode material and its nanostructure are the keys to boost the response frequency of an EC from below 1 Hz to above 1 kHz. In this Review, we summarize guidelines on the electrode nanostructure design for kHz response, discuss the various carbonaceous materials and other highly conductive materials based electrode structures for kHz ECs. The configurations of higher voltage kHz ECs, and their dimension advantage over AECs are critically evaluated, followed with the outlook on the further study and development in this promising area.

1. Introduction

ECs, particularly those based on double layer capacitance (DLC), are being applied as low-density energy sources, or as power buffer assisting batteries. As energy source, these commercially available devices run at direct current (DC). They cannot be charged and discharged at a frequency more than 1 Hz or so, due to the complex micropore network in the electrode that gives large electrochemical resistance.[1-3] Another category, pseudocapacitance based ECs are even slower than DLC based owing to the intrinsic slow charge transfer process across the electrolyte/electrode interface.

In contrast, electrolytic capacitors [4-6] are a type of polarized asymmetrical dielectric capacitor. On a roughened metal surface that provides a large surface area, an extreme thin metal oxide is anodically grown. This oxide layer, acting as the dielectric material and therefore determining the rating voltage, is then sandwiched between the original metal base as the anode and an electrolyte, with the electrolyte further contacted with a cathode. The polarity is caused by the electrochemical decomposition of metal oxide under a reversed voltage. Electrolytic capacitors have a lower capacitance density by several orders of magnitude than ECs, but they can response up to ~ 10 kHz or higher frequencies. They are very suitable, as circuit element, for passing or bypassing low-frequency signals, widely used for ripple and noise filtering and decoupling in power supplies, DC link circuits, power factor correction, photo flashing and strobe, among others. This is particularly true for aluminum electrolytic capacitors (AECs) when filtering current ripples. For 60 Hz line frequency, the filtering capacitor, following the full-wave rectifier, must response at 120 Hz and with minimum loss (thermal generation). At such frequency, conventional ECs would have lost their capacitive characteristic, instead, it behaves like a highly lossy inductor with a positive impedance phase angle. Therefore, such ECs cannot be used as circuit elements for filtering, decoupling, and other functions.

Nowadays, with the progress of semiconductor technology, discrete passive components, especially AEC filtering capacitors, play critical roles in determining the circuit board profile, reliability, power conversion efficiency, among others. AECs, even for a small capacitance on the order of μF, have bulky sizes which is a limiting factor in the down scaling of circuit boards, particularly for portable electronics. An interesting question then arise: can ECs, with a much compact size and small ESR, be made faster to replace the bulky AECs?

In a second frontier, with the rising of internet of things (IOT) and autonomous sensor network, the unattended micropower sensor need to harvest environmental mechanical energy through piezogenerator or tribogenerator for self-powering.[7] Since most environmental noise or vibration has a dominant frequency in the range of tens to hundreds hertz, the micro-generators produce pulse power in this frequency range. Again, conventional slow ECs are not efficient for storing such pulse power, while

AECs are simply too bulky to fit in a tiny senor module. A compact kHz EC provides an ideal solution for storing such pulse power form environmental energy harvesting.

Major research efforts on ECs have been concentrated on improving their energy density to bridge the energy density and power density gap between ECs and batteries. On the other hand, there is also a performance gap, in terms of capacitance density and frequency response between ECs and electrolytic capacitors (Figure 1a), while bridging this gap clearly will have great impacts on compact circuit design and self-powered tiny sensor system (Figure 1b).

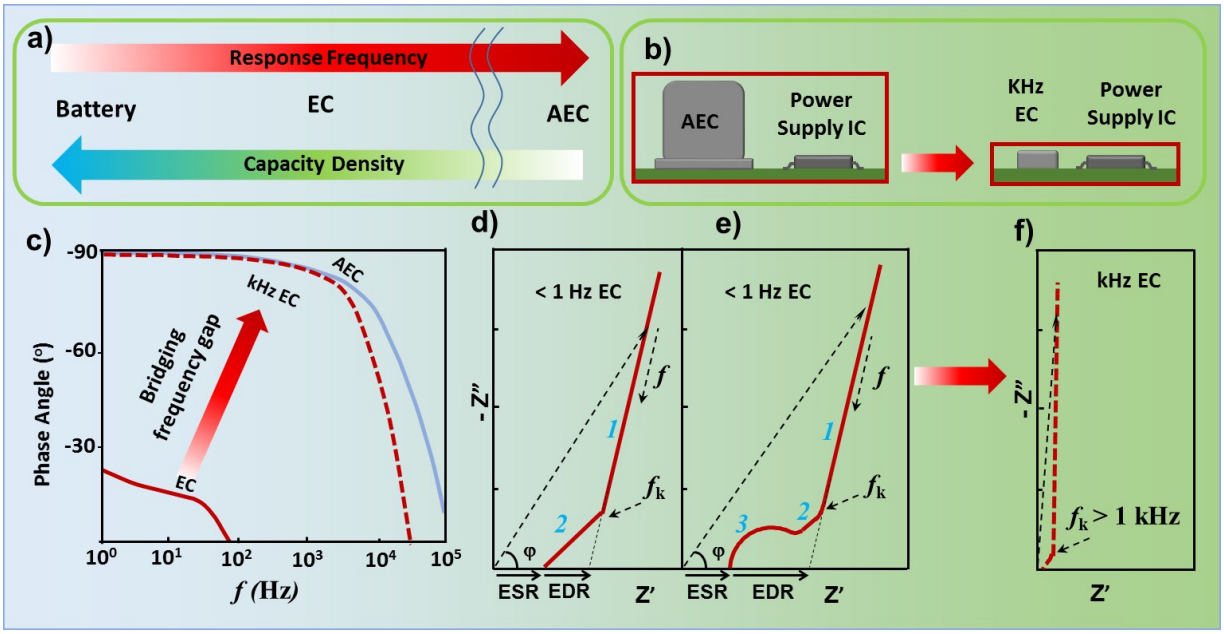

Figure 1. (a) The performance gap between battery, EC and electrolytic capacitor in terms of response frequency and capacitance density. (b) Using kHz EC to replace bulky AEC for compact circuit design. (c) EIS Bode plot illustrating the performance gap in term of frequency response between the conventional EC and AEC, and how the kHz EC bridging this gap. The characteristic regions in the EIS Nyquist plot for conventional EDLC in (d) and of pseudocapacitor in (e) and those of kHz ECs in (f).

Since the pioneering work of Miller *et al.* on demonstrating the first kHz range EC,[1] a strong interest in this area have resulted in dramatic progress in developing high-frequency ECs,[8-18] to replace AEC or find new functions in power electronics, power supply and energy harvesting. As illustrated in Figure 1c, an "ideal" kHz EC will bridge the huge performance gap, in term of frequency response, between the conventional slow EC (< 1 Hz) and bulky AEC.

To further promote the research interest on developing an 'ideal" kHz EC, we review the past efforts and current status of high frequency ECs. Section 2 highlights the major factors restraining the high-

frequency response of conventional ECs and provides general guidelines on the electrode nanostructure design for kHz response. Section 3 reviews the varieties of sp^2 carbonaceous materials based electrode design for EDL based kHz ECs. Section 4 explores other highly conductive electrode materials from which some are based on the pseudocapacitive effect. Section 5 discusses the configurations of higher voltage kHz ECs and makes predictions on their dimension advantage over AECs. The last section concludes with an outlook on the further areas of study.

2. Characteristic Frequency Response and Nanostructure Design Guidelines

Understanding the fundamental mechanisms governing the frequency response of ECs will provide guidelines on the electrode nanostructure design toward the development of kHz ECs. Electrochemical impedance spectroscopy (EIS) is commonly used to analyze their frequency response.[19,20] As schematically illustrated in Figure 1d,e in most cases, the Nyquist-plot of EIS spectra contains features of: 1) a tilted but close to vertical line at low frequency, which can be modeled as a constant phase element (CPE) with an ideality factor. 2) Towards higher frequency, a knee point (knee frequency f_k) appears, followed by the characteristic 45° slope region, a result of distributed capacitance and resistance in a porous electrode. 3) When an insulating layer covering the current collector or when pseudocapacitive effect exist in the electrode, following or merging with this region at higher frequency range is a typical semicircle feature (Figure 1e).[21] Because of the three features of EIS spectrum, the absolute value of the phase angle φ at high frequencies is therefore much less than the ideal 90°. Equivalent series resistance (ESR) is commonly defined as the resistance value when the impedance curve intersects with the Z'-axis. However, this parameter is not sufficient to evaluate the frequency response, since the characteristic 45° slope region and the semicircle region can lead to a very small ESR but a sluggish response. When using a simplified RC model to estimate the time constant, the resistance value R, the extrapolated intersection of the near-vertical linear section of EIS with the Z'-axis should be used. Therefore, equivalent distributed resistance (EDR) can be defined as the difference between this R value and the ESR (Figure 1d,e), to evaluate the adverse effects of the characteristic 45° slope region and the semicircle region on the frequency response.

To have a high-frequency response with a minimum loss (Figure 1f), a small ESR is essential. This requires minimizing the electrolyte resistance, the electrode material resistance, and the contact resistance between the electrode material and the current collector. To behave like an ideal capacitor at high frequencies, a large f_k is needed. This demands eliminating the semicircle feature and minimizing the distributed capacitance and resistance region if the later one cannot be completely eliminated, thus achieving a small EDR.[22,23] A minimized distribution region means distributed charge storage, related to

porous effect,[24] should be diminished. The transmission line model (TLM) has been commonly applied to simulate the distributed charge storage effect.[24] The modification of TLM by incorporating pore size distribution function, have also been applied to simulate the relationship between pore structure and frequency response, and successfully explained how pores length and pore radius of electrode materials, electrolyte conductivity, and others can affect capacitance and dynamic response.[25] A few guidelines on electrode design towards kHz ECs are summarized as:

- Highly conductive electrode material, and probably in an intimate interconnected format with minimum internal resistance. Particulate materials should be avoided due to large inter-particle resistance, and thus those structures composed of intrinsically connected 2D (graphene) or 1D (carbon nanotube array) are good candidates.
- A minimum contact resistance with the current collector. Electrode material should be directly grown on the metal foil or coated on by adopting particular interface morphology or interlayer.
- Ultrathin (~ 1 μm) or thin (~ 10 μm) electrodes to minimize the porous effect.
- Well-connected and large-size pores should be used, and particularly avoid micropores, dead pores, and tortuous pore geometry. The choice of pore diameter strongly depends on the ionic conductivity of the electrolyte.[24,25]

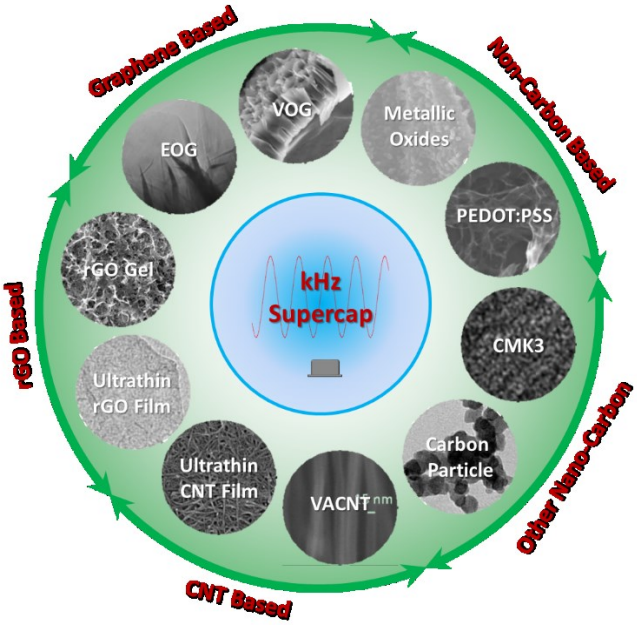

Figure 2. Representatives of different carbon based and non-carbon based nanostructures used for developing kHz ECs.

In term of frequency response, a figure of merit is the frequency when the impedance phase angle reaches −45° since this is the frequency defining the boundary between the capacitive and the resistive behavior of the cell. Here, we define this frequency as the cutoff frequency f_0 of the cell. The so-called relaxation time constant, defined as $\tau_0 = 1/f_0$ is another merit parameter. For line frequency applications, the phase angle at 120 Hz (φ_{120}) is critical and should be close to the ideal value of −90°. On the other hand, since the whole purpose of developing high-frequency EC is for a compact size, the single-electrode areal and volume capacitance densities (C_A and C_V) at 120 Hz are critical parameters.

Tailoring the porous structures to simultaneously achieve high frequency response and large capacitance density is the key in developing kHz EC technologies. Figure 2 illustrates the representative materials and their nanostructures that have been investigated for the development of kHz ECs.

3. Carbon Based Electrodes

Due to their electrochemical inertness and low cost, different types of carbon materials such as activated carbon and carbon black that offer a large specific surface area (>1000 m^2 g^{-1}), have been commonly used as EC electrodes.[26] But their tortuous micropore structure and low electrical conductivity restrain their frequency response to below 1 Hz.[19] Considering the intrinsic high conductivity of carbon nanotube (CNT) and the well-opened pore structure in CNT membranes, it is not surprising that pioneering works on fast ECs started from CNTs in the 1990s, when huge interests were attracted to this nanomaterial. Using CNT membranes, Niu *et al.*[27] reported in 1997 for the first time an EC with a knee frequency of 100 Hz and a capacitance of 49 F g^{-1} at 100 Hz. But the demonstrated cell still had a very low cutoff frequency of only 6 Hz.

Following this unprecedented result, strong interests were attracted to develop CNT-based electrodes for high power density and high-frequency response.[28,29] A significant improvement was reported by Pan's group,[30,31] when thermally treated CNT films in hydrogen were used as electrodes that had a dramatically reduce ESR by eliminating the oxygen-containing species on the CNTs. Such cell exhibited a knee frequency 7.65 kHz and a cutoff frequency ~ 500 Hz. The phase angle at 120 Hz was –65°, which was still far short for line-frequency applications.

With the excitement on graphene in the 2000s, the breakthrough on kHz range ultrafast ECs that are suitable for line-frequency filtering was finally reported by Miller *et al.* in 2010,[1] who used vertically oriented graphene (VOG) films deposited by plasma-enhanced vapor deposition (PECVD)[32] on a metal substrate as electrodes to achieve very fast response with a cutoff frequency 15 kHz and a relaxation time of 0.067 ms. This pioneering work suggested, for the first time, the promise of developing kHz ECs with a compact size in replacing AECs for current filtering. Since then, huge interests have been attracted into

this new field of developing kHz ECs for electrical circuit applications, different from the efforts on high energy density ECs as energy storage. This burgeoning field has achieved a steady progress. In the following, we review the different carbon based nanostructures suitable for kHz ECs.

3.1 Graphene based structures

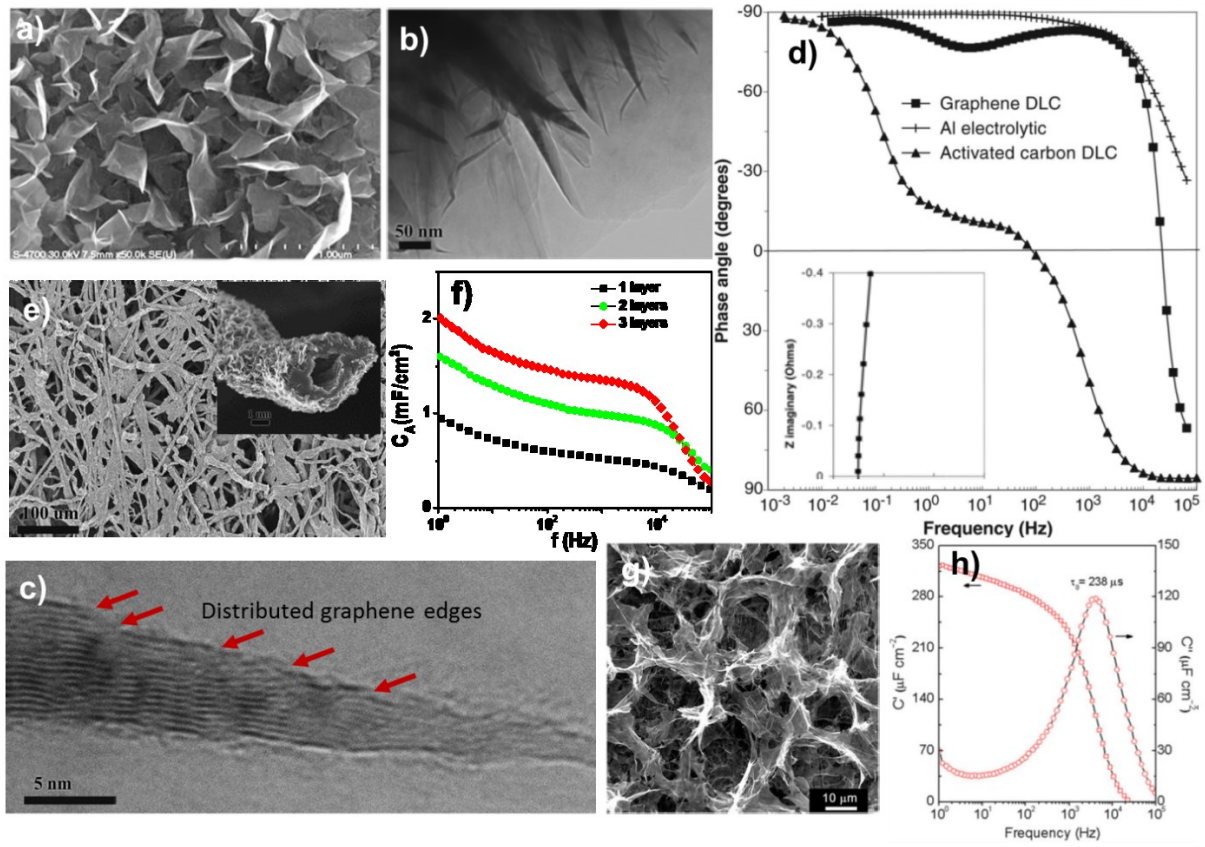

Figure 3. (a) SEM and (b, c) TEM images of VOG flakes. (d) Impedance phase angle versus frequency for the VOG cell, in comparison to an activated carbon EDLC and an AEC. Inset is a complex plane plot for the graphene EDLC. (e) SEM image of EOG/CCP network, and inset is EOG coated single carbon fiber. (f) Electrode performances based on 1, 2, and 3 layers of EOG/CCP sheets. (g) SEM image of oriented rGO aerogel, and (h) plot of the real or imaginary part (C′ or C″) of specific capacitance versus frequency for the electrode in (g). Reproduced with permission from Ref. 1 for (a,d), Copyright 2010, and Ref. 8 for (g,h), Copyright 2012, The American Association for the Advancement of Science; Ref. 12 for (b,c,e,f), Copyright 2016, Elsevier.

Vertically oriented graphene or thin-graphite (VOG), or more generally edge oriented graphene (EOG) when considering 3D cases, can be grown on a substrate or inside a 3D foam via a PECVD process using methane or other hydrocarbons as precursors.[33-35] The salient features of VOG or EOG (Figure

3a,b), such as the fully exposed graphene edges, pore structure with straightforward, short, and relatively large pores, its high electronic and electrolyte ionic conductivity, and trivial interface resistances between interconnected VOG flakes and between VOG and the underlying current collector, make it very suitable for kHz ECs. Each VOG flake, consisting of multi-layer graphene, has a tapered profile with easily-accessed, fully-exposed and high-density graphene edges (Figure 3c).[36,37] These edges or steps have an electrochemical reactivity several orders of magnitude higher than its basal plane due to a large amount of defects that produce a high density of defect states near the Fermi level.[38,39] These atomic edges or steps are also the potential adsorption sites of electrolyte ions. Although precise areal capacitance values are not accepted universally due to the measurement technique, edge plane double layer capacitance has been reported to be 50 to 70 mF cm^{-2} in contrast to a mere ~3 mF cm^{-2} from the basal plane.[40] Irrespective of the exact values, exposed graphene edges of VOG would clearly augment achievable capacitance of kHz electrochemical capacitors.

In the pioneering work of Miller *et al.*,[1,32] 0.6 μm VOG was deposited on Ni substrates as electrodes in a PECVD process. The symmetric cells with KOH electrolyte exhibited cutoff frequency of 15 kHz, close to a conventional AEC (Figure 3d). EIS spectra showed a vertical intersection with the real axis due to the straightforward channels between flakes. At 120 Hz, an electrode areal capacitance was about 0.175 mF cm^{-2}. It was estimated that VOG stored ~1.5 FV cm^{-3} with the aqueous electrolyte (0.5 V) and ~5.5 FV cm^{-3} with the organic electrolyte (1.25 V), in contrast to a typical AEC with a value of ~ 0.14 FV cm^{-3} only. Assuming the thickness of each electrode as 7 μm, and the separator as 10 μm, VOG EC has a larger capacitance than AEC for a voltage up to 15 V.[32] Following this work, further studies along this line of research were reported.[41,42] Particularly Cai *et al.*[9] optimized VOG growth on Ni substrate, achieving a cutoff frequency of 20 kHz, 120 Hz phase angle of – 85°, and areal capacitance as large as 0.265 mF cm^{-2}.

Recently, VOG has been grown on Al substrate for fast ECs.[43] Defect generation in VOG using Ar plasma was reported, indicating a change in the density of states near the Fermi level with increased defect density, and hence a corresponding increase in electrochemical capacitance capability.[44] Defect generation may also enhance the wettability of VOG in aqueous electrolytes for higher capacitance. It was also reported that graphene intersheet distance plays a critical role on the wettability of VOG and reducing the sheet distance will enhance the wettability. A 3-fold improvement in the accessible surface area of VOGs was achieved by reducing intersheet distance.[45] In a comprehensive experimental and simulation study, edge effects of VOG were reported.[46,47] Compared to the basal planes, the edges present higher initial charge density (by 4.2 times), higher ion packing density (by 2.6 times), closer ion packing

location, and larger ion separation degree. These findings provide useful guidelines in guiding VOG structure design to enhance kHz EC performances.

In all these studies of VOG grown on a 2D flat substrate, a restricted VOG film thickness (~ 1 μm) and a low graphene flake density (for wide pore channels) put a limitation on its area specific capacitance. Filling carbon black nanoparticles into the porous channels between VOG flakes was tested for a larger areal capacitance,[10] but this approach might severely restrict the frequency response. For an enhanced areal capacitance, EOG was deposited in 3D Ni foams with EOG flakes encircling scaffolds with perpendicular orientation,[11] in contrast to laterally oriented growth.[48,49] With folded EOG inside the foam, more EOG flakes can be deposited on the same foot print, and thus an electrode areal capacitance of 0.72 mF cm^{-2} at 120 Hz and 0.32 mF cm^{-2} at 1 kHz was achieved, with a cutoff frequency of 4 kHz.[11] Ni foam also can be etched off leaving freestanding EOG foam as electrode with much less of mass and thickness after compression.[36] However, the pore size of Ni foam (50 – 100 μm) is too larger for the EOG (~ 1 μm). Recently, EOG growth in Al foam with several micrometer pore size was reported where Al foam was produced by etching Al foil in NaOH solution.[50] Although the demonstrated cell has limited rate performance, probably caused by the tiny pore size in Al foam, this study does suggest an approach to tune the metal foam[51] pore structure for better EOG electrode fabrication.

We recently reported 10 μm thick flexible freestanding electrodes, formed by EOG grown radially around individual carbon fibers in carbonized cellulose paper (CCP).[12] Cellulose fiber carbonization (graphitization) and EOG deposition was implemented in one 5-mintues high-temperature plasma processing step. The microscale morphology of EOG/CCP electrodes are shown in Figure 3e. Such free-standing electrodes based on a single EOG/CCP sheet (10 μm total thickness) had a large electrode areal capacitance of 0.59 mF cm^{-2} with a phase angle of -83^{o} at 120 Hz. Particularly, the hierarchical EOG/CCP sheet structure allows multiple sheets to be stacked together for thick electrodes with almost linearly increased areal capacitance, while maintaining the volumetric capacitance with nearly no degradation, a critical merit for developing practical large capacitance kHz ECs. 3-layers of EOG/CCP electrode (30 μm thick) achieved an areal capacitance of 1.5 mF cm^{-2} and particularly a volumetric capacitance of 0.5 F cm^{-3} at 120 Hz, when the whole volume of the electrode (including current electrode) was considered. Furthermore, these EOG/CCP electrodes exhibited highly stable performance. After continuing test for 200,000 cycles, the capacitance had no degradation, instead it was slightly increased. The slight increase of capacitance was caused by the expansion of the interlayer space of multilayer graphene flakes.

Although most demonstrations of VOG based kHz ECs were based on aqueous or organic liquid electrolytes due to their high ionic conductivities, solid-state kHz ECs with ac line-filtering capability were also reported for better stability and longer lifetime, where tetraethylammonium hydroxide

(TEAOH)-polyvinyl alcohol (PVA) based polymer electrolyte was used.[52] For the sandwich-type cell configuration at 120 Hz, the impedance phase angle of −81°, and capacitance of 0.086 mF cm^{-2} was obtained. Also, solid-state planar interdigitated cells with high frequency response was demonstrated. These solid-state cells, even with limited packaging, retained high performance over 18 months of shelf storage and after 100,000 charge/discharge cycles, confirming the high stability of TEAOH–PVA electrolyte and VOG electrode. VOG grown on metallized silicon nanocone array was also reported as electrodes in cells with gel electrolyte, but the frequency response was low.[53]

So far, all the VOG or EOG electrodes for kHz ECs were produced in a PECVD process to achieve intimate connection between graphene flakes and between graphene and the current collector. These electrodes offer superior frequency response, but the PECVD process may limit the achievable electrode size. Other cost-effective methods for producing VOG or EOG structures should be explored, although its morphology and particularly the packing density of graphene sheets might be very different.

A unique method to fabricate vertically oriented graphene based on reduced graphene oxide (rGO) was reported.[54] Using chemically derived graphene oxide (GO) nanosheets as the precursor, highly dense and vertically oriented rGO electrodes were produced via simple hand-rolling, cutting and thermal reduction processes. Such electrodes exhibited large volumetric and areal capacitance and fast electrolyte ion diffusion property. ESR and porous electrode behavior of these electrodes are much diminished when comparing to randomly oriented rGO electrodes, and particularly a cutoff frequency of 810 Hz was obtained. Owing to a large packing density of rGO nanosheet, distributed charge storage caused by porous effect is one major reason limiting its frequency response. It is expected that if the packing density is reduced to enlarge inter-sheet spacing, higher frequency response and larger phase angle might be achieved through the minimization of distributed porous electrode behavior. Minimizing the inter-sheet resistance is also important.

Another approach based on a salt-templating method to fabricate EOG structures was also reported, although it was not for EC study.[55] In this method, ionic liquid carbon precursor was mixed with salt mixture ($ZnCl_2$ and KCl) and casted into Ni foam. After thermal treatment in an inert gas and subsequently removal of salts by washing, EOG structures were obtained. After tailoring the sheet density and height, such a structure might also be useful for kHz ECs.

In addition to VOG or EOG structures, porous graphene (or rGO) aerogel was investigated for kHz ECs. Graphene aerogel is characterized with a 3D porous network,[56-59] allowing most of the sheets exposed to the electrolyte. Its largely opened pores can facilitate the unobstructed transportation of electrolyte. Shi's group[8] reported using electrochemical reduction of GO nanosheets on Au foil as kHz EC electrodes. Electrochemical reduction ensures rGO flakes to be quasi-vertically aligned on the metal

foil, forming macro-size and vertically oriented pore structure (Figure 3g). They were further reduced in $LiClO_4$ aqueous solution to increase the conductivity, and then freeze-dried. The electrode demonstrated a high-frequency response. The impedance phase angle was -84° at 120 Hz, and the cutoff frequency was 4.2 kHz. The Nyquist plot was nearly a vertical line, reflecting its high conductivity and rate capability. An area capacitance of 0.28 mF cm^{-2} for the cell and a relaxation time constant of 0.238 ms (Figure 3h) were achieved.

Aiming at high-power ECs but not particularly for kHz high frequency, many studies were conducted using rGO aerogel,[60-62] of which most used aerogel structures with rGO flakes laterally oriented. The consequence is that the laterally orientated rGO sheets might block the rapid transportation of electrolyte in the vertical direction for a sandwich-type cell, resulting in sluggish frequency response. Therefore, vertical alignment of rGO in the electrochemical reduction process is the key to the high frequency response demonstrated in Ref. [8].

To facilitate ion transportation through the lateral graphene sheets, the strategy of using ultrathin film was explored. The frequency response of an EC is strongly related to the transportation of both the electrolyte ions and electrode electrons across the whole thickness of the electrode material layer. Therefore, the active material thickness is a critical parameter in determining their rate capability. Ultrathin graphene films, with a thickness of less than ~ 100 nm are a strong candidate for kHz ECs, even though they do not have the oriented or much large-size pores.

Shear exfoliation is promising for few-layer graphene manufacturing. Paton *et al.* [63] investigated the method of shear exfoliation of graphite in liquids without pre-intercalation[64] for scalable production of large quantities of defect-free few-layer graphene. They further demonstrated that using the highly conductive graphene thin films with a thickness of 25 nm for ultrafast ECs. The exfoliated graphene nanosheets have sizes in the 300–800 nm range with typical thicknesses of less than 10 monolayers per nanosheet. Ultrathin graphene films with a conductivity as high as 400 S cm^{-1} were prepared via vacuum filtration and slightly annealing. In a three-electrode cell, the 25 nm thick graphene film electrode showed excellent frequency response and capacitance density. At 120 Hz, the impedance angle was –79° but with a very small capacitance of 0.035 mF cm^{-2} due to the small amount of material used. Wu *et al.* reported ultrathin printable graphene ECs.[65] A conductive ink of electrochemically exfoliated graphene[66] and poly(3,4-ethylenedioxythiophene):poly(styrenesulfonate) (PEDOT:PSS), was spray-coated on 2.5 μm Au/PET substrate, with a thickness of tens of nanometers. These much thin electrode are highly flexible. Polymer gel electrolyte of H_2SO_4/PVA was employed, sandwiched by two thin electrodes. For electrodes with active material thickness of 25 nm, 77 nm, and 128 nm, the cutoff frequencies at –45° are 1 kHz, 708 Hz, and 320 Hz, respectively. The phase angle for these electrodes are around – 75° at 120 Hz.

Blocking of the ion transport in the vertical direction by lateral graphene nanosheets restricts the high-frequency response, particularly for thicker electrodes.

Although ultrathin (< 100 nm) graphene films show reasonable frequency response,[65] the small graphene loading results in low areal capacitance density. To have enough material loading (thickness) and to facilitate rapid ion transport in the vertical direction simultaneously, Shi's group reported the strategy of using holy rGO nanosheets that were further doped with nitrogen.[13] Starting from GO/Fe_2O_3 nanorods/polyvinylpyrrolidone (PVP) hybrid gel, the holy graphene films were prepared via doctor-blade coating, followed by thermal annealing and acid treatment. Fe_2O_3 nanorods catalyzed the pore etching and the decomposition of PVP led to N doping into rGO. Nitrogen doping enhanced the conductivity and hydrophilicity, while the etched holes in rGO sheets, acting as ion transport channels, ensure the fast response of the electrodes. The electrode exhibited high areal and (active material based) volumetric capacitance of 0.956 mF cm^{-2} and 1.2 F cm^{-3} at 120 Hz, respectively, with a phase angle of –81.2°.

3.2 CNT based structures

As previously introduced, CNT membrane was the first electrode material studied towards fast ECs. After the pioneering work by Niu *et al,*[27] considerable progress was made by Pan's group[30] resulting in fast ECs with a cutoff frequency ~ 500 Hz.

Following the design guidelines summarized in Section 2, reducing CNT film thickness becomes necessary in order to further improve the response frequency into kHz range. Several studies were reported using sub-μm thick CNT films as electrodes. Since CNTs are dispersed on a current collector, Au-coated metal was typically used to minimize the contact resistance. In Tang's study,[17] single-wall CNT (SWCNT) mesoporous thin film, with a mass loading of 19.9 μg cm^{-2}, exhibited a cell capacitance of 0.6 mF cm^{-2}, a phase angle of -81° at 120 Hz, and a cutoff frequency of 1.4 kHz. However, the mesoporous structure rendered a low value of the phase angle at frequencies below 10 Hz. Although a thicker film (138 μg cm^{-2}, ~ 1.6 μm) can increase the capacitance by several times, the frequency response is severely restrained with a phase angle close to -50° at 120 Hz.

Similarly, in the study from Kim's group,[15] ultrathin SWCNT films with thickness from 53 nm to 298 nm, with the corresponding mass loading of 5 to 32 μg cm^{-2} were investigated, but with tetraethylammonium tetrafluoroborate ($TEABF_4$) dissolved in acetonitrile as the electrolyte. Single kHz cell running at 2.5 V was demonstrated for the first time. For the 32 μg cm^{-2} mass loading, a cell capacitance of 0.28 mF cm^{-2} (25.5 mF cm^{-3}) and -82° phase angle was demonstrated at 120 Hz with a cutoff frequency of ~ 2 kHz. The same group further progressed with a demonstration of 3V solid-state flexible kHz ECs using ionic-liquid-based polymer gel electrolyte (Figure 4a-c).[16] Gel electrolytes were

prepared by mixing the poly(styrene-block-ethylene oxide-blockstyrene) (PS−PEO−PS) triblock copolymer and 1-ethyl-3-methylimidazolium bis-(trifluoromethylsulfonyl)imide in acetonitrile. The cyclic voltammogram (CV) is almost rectangular at high scan rate (300 V s^{-1}) for a typical cell with up to 3 V potential window. The fabricated cells based on CNT electrode and ion-gel electrolyte exhibited a fast frequency response that depends on the thickness of both CNT film and gel separator. With CNT film from 300 nm (~32 μg cm^{-2}) to 50 nm (~4 μg cm^{-2}), the 120 Hz phase angle increases from -70.6° to -82.7°, but the cell capacitance decreases from 0.233 to 0.043 mF cm^{-2}. Notably, this study also demonstrated that assembled kHz cells can be used in an AC filtering circuit for the conversion of 60 Hz AC input into DC output. A full-bridge diode rectified the AC input wave of ±4.3 V at 60 Hz into pulses of 0−3.2 V at 120 Hz. The rectified pulses were then filtered by the cell to obtain smooth DC voltage (~ 2.9 V) without ripple noises. Such result is very encouraging in developing compact kHz ECs for such filtering applications.

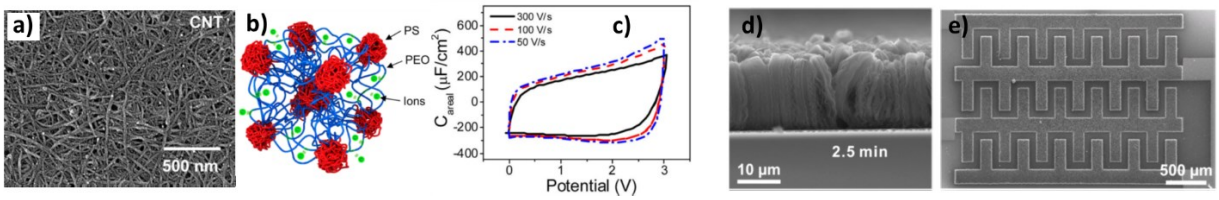

Figure 4. (a) SEM image showing the surface morphology of the CNT ultrathin film. (b) Schematic illustration of the ion gel. (c) The CV curve showing the 3V potential window. (d) SEM image of VACNT grown for 2.5 min, and (e) the interdigitated electrode pattern of VACNT. Reproduced with permission from: Ref.16 for (a-c), Copyright 2016, and Ref. 67 for (d,e), Copyright 2013, American Chemical Society.

Following the same concept of VOG grown on a metal current collector that can offer a high frequency response, vertically aligned CNT (VACNT) grown on a metal foil should be ideal for kHz UECs. VACNTs grown directly on a metal current collector were investigated before the reporting of VOG electrodes. One early study showed a cutoff frequency of 443 Hz.[68] In another study, ~ 200 μm thick VACNT films were grown on a Si substrate, and then transferred to an aluminum current collector.[69] With $TEMABF_4$/PC electrolyte, the assembled cell at 1 kHz exhibited a capacitance of ~ 60% of its DC capacitance. The aligned CNTs provide oriented and regular pore structure to facilitate ion transportation. However, the dense packing of CNTs, and particularly the thick film leading to deep narrow pores result in obvious porous electrode behavior with the characteristic transmission-line-like response.[70-72] Also, the

thick films increase the resistance of the electrode material significantly. Therefore, their cutoff frequency was much less than 1 kHz.

The effect of VACNT film thickness was investigated using planar interdigitated electrode configuration. VACNT based micro-ECs with excellent frequency response and capacitance density was reported (Figure 4d,e).[67] VACNTs grown for 1, 2.5, and 5 minutes with thickness of ~ 5, 10, and 15 μm were studied. At 120 Hz, the phase angle was −81.5° for the 1 min sample and reduced to −73.4° for the thick CNT grown for 5 min. Their cutoff frequencies were ~1343, 754, and 460 Hz, respectively. A very informative work using VACNTs was reported by Lee's group,[25] who experimentally demonstrated and theoretically modeled the frequency response of VACNT electrodes in a planar configuration. Transmission line model combined with information of pore size distribution was used to simulate frequency response. A systematic study of the dependence of relaxation time constant on pore length and diameter, the CNT density, electrode thickness, and electrolyte conductivity was reported. They also compared the frequency response of VACNTs, and randomly oriented CNT films.

3.3 Other carbon based structures

Unlike graphene and CNT, carbon black is considerably cost effective when considering large-scale production. Commercially available SC3-type carbon black has short pores with fast accessibility by electrolyte ions, potentially allowing fast frequency response operation. Kossyrev[73] reported that for ~ 1 μm thick SC3 carbon black coated on the conductive vinyl current collector, a phase angle of −75° at 120 Hz was demonstrated with a cutoff frequency of 641 Hz. This carbon black based electrode, after further improvement, might provide an economic approach to produce practical kHz ECs.

Different from the ultrathin films, carbon sponges with mass loading of 1.5 mg cm^{-2} were also investigated.[74,75] The sponge showed a bimodal pore-size distribution, with mesopores and macropores. The assembled coin cells exhibited reasonable high-frequency response with a phase angle of −78°, a cell capacitance of 0.17 mF cm^{-2} at 120 Hz, and a cutoff frequency of 4.2 kHz.

A sandwich-type structure, with an ultrathin amorphous carbon film sandwiched from both side by multilayer graphene films, was obtained in a CVD process by decomposing methane on a nickel substrate, thus achieving thickness-controllable freestanding hybrid carbon films.[76] At 120 Hz, the impedance phase angle for the film electrode with a thickness of 1.12 μm was approximately −67°, with cutoff frequency ~7 kHz. Similarly, 3D foam-like carbon materials were synthesized by CVD deposition into Ni foam, followed by Ni etching off.[77] For the structure grown at 600°C, a phase angle of −78° and an electrode capacitance of 0.1 mF cm^{-2} at 120 Hz was found with a cutoff frequency of 17 kHz.

Ordered mesoporous carbons are interesting materials for electrochemical energy applications due to their well-defined pore size and pore regularity.[78,79-81] Kim's group[18] demonstrated that graphitic ordered mesoporous carbon could be used for kHz ECs. CMK-3 particles with widely opened pore structure, and graphitic crystalline domains, are mixed with SWCNTs, and coated into thin films. Tested with $TEABF_4$ based organic electrolyte, a 120 Hz phase angle of ~ -80^o, and a cell capacitance of 0.56 mF cm^{-2} were achieved with a cut off frequency of ~ 1 kHz being found. Since the demonstrated CMK-3/CNT cell has a volumetric capacitance of 50.2 F cm^{-3}, it was further estimated that up to ~ 41 V, such electrode based ECs have a more compact size than the commercial AECs.

At the end of this section on carbon materials based electrodes, we mention that in addition to sandwich-type cell studies we emphasized here, there are also many reports on the interdigitated electrode based planar-type cell[82-86] studies with high frequency response.[87-90] We also emphasize that there are considerable efforts in developing carbon based electrode nanostructures, using highly conductive graphene, CNT, and other sp^2 carbon materials[91] to form nanostructures or nanocomposites with considerable large surface area, which offer reasonable high charge-discharge rate and high capacitance density, thus a much larger power density than the conventional ECs.[92-109] Since these electrode structures are not designed particularly targeting at high frequency (>100 Hz) applications, they are not directly adapted for the kHz ECs discussed here used for AC filtering. However, some of these structures[110-120] showed reasonable frequency response (tens of Hz). With suitable modification by trading-off between speed and capacitance, they might also be useful for design of kHz EC electrodes.

4. Other Active Electrode Materials

In contrast to sp^2 carbonaceous electrodes for kHz EC development, which are based on double layer capacitance, several interesting studies were reported using other conductive materials, which are reviewed in this section. Highly conductive diamond foam, deposited on sacrificial SiO_2 particle layer by PECVD, was studied.[121] In aqueous electrolyte and organic electrolyte, the thin-film porous electrode showed relaxation time constant of 3.16 ms and 6.20 ms, respectively, but with small DC capacitance less than 0.1 mF cm^{-2}. Highly-doped conductive silicon nanotrees (nanowires with branches), through 3-step CVD deposition, were also investigated.[122] Using organic electrolyte, the device exhibited a relaxation time constant of ~ 9 ms, but again with a small DC capacitance less than 0.1 mF cm^{-2}.

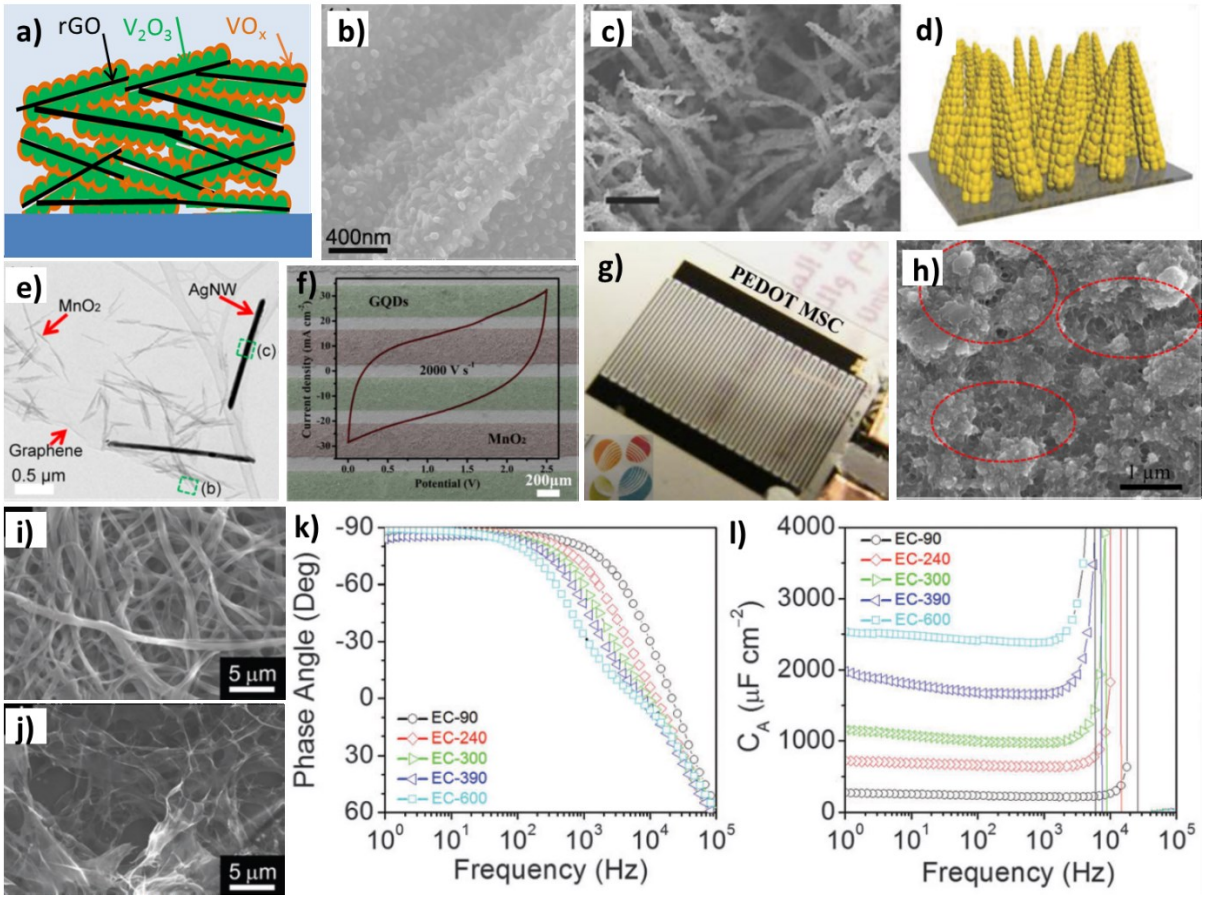

Figure 5. (a) Schematic and (b) SEM image of rGO bridged V_2O_3/VO_x core-shell composite as an electrode for fast pseudocapacitors. (c) SEM image and (d) schematic of corn-like TiN nanostructures for fast pseudocapacitors. (e) TEM image of rGO/MnO_2/Ag-NW hybrid film, with need-like MnO_2 and Ag-NW bridged with rGO sheets. (f) CV scan at a rate of 2000 V s^{-1} for GQD//MnO_2 asymmetric cell. (g) Optical photograph of PEDOT based micro-EC, and (h) SEM image of porous PEDOT electrodes. (i) SEM image of PEDOT:PSS coated cellulose paper, (j) SEM image of acid-treated porous PEDOT:PSS film, (k) phase angle vs. frequency, and (l) areal capacitance vs. frequency plots for treated PEDOT:PSS electrodes with different thickness. Reproduced with permission from Ref. 123 for (a,b), Copyright 2014, and Ref. 124 for (c,d), Copyright 2015, John Wiley and Sons; Ref. 125 for (e) and Ref. 126 for (f), Copyright 2015, American Chemical Society; Ref. 127 for (g,h), Copyright 2016, American Chemical Society; Ref. 14 for (i-l), Copyright 2015, Royal Society of Chemistry.

More interesting studies are those investigating electrochemically active materials for fast and ultrafast ECs that combine both double layer capacitance, and pseudocapacitance effects. Transition

metal oxides, nitrides, chalcogenides, and conductive polymers are widely investigated to explore their larger pseudocapacitance for high energy-density ECs. Charge transfer based pseudocapacitive effect is intrinsically slow. However, by exploring some particular oxides, nitrides, chalcogenides, or polymers with high conductivity, several studies reported unexpected and exciting results. To compensate for the low conductivity of these materials, highly conductive graphene or similar carbon based scaffolds are often adopted to coat the pseudocapacitive materials.[128-130] However, we cautiously point out that at high rates, particularly working at hundreds of Hz, whether the charge transfer reaction does occur probably should be further investigated.

Transition metal oxides based electrodes typically work at a charge-discharge rate in the range of mV s^{-1}. To overcome the low conductivity challenge for rapid pseudocapacitor design, graphene bridged V_2O_3/VO_x core-shell composite was reported as electrode structure (Figure 5a,b).[123] Metallic V_2O_3 nano-cores were dispersed on rGO sheets for electrical connection, while a naturally formed amorphous VO_2 and V_2O_5 thin shell around V_2O_3 nano-core acts as the active pseudocapacitive material. Thermal treatment in H_2 significantly improved the performance.[131] With such a nanostructure electrode, ECs with a charge-discharge rate as high as 50 V s^{-1} were demonstrated, offering 1 MW kg^{-1} power density at an energy density of 10 Wh kg^{-1}. The high rate and high power capability were attributed to the largely enhanced conductivity of this unique structure and a possibly facile redox mechanism. EIS measurements confirmed a cutoff frequency of 114 Hz at −45° phase angle.

Metal nitrides are another category materials with high conductivities that can be explored. Metallic titanium nitride (TiN) is a good candidate.[132] Corn-like TiN nanostructures were grown on nanoengineered metal substrates using atomic layer deposition. Thus formed TiN film has a particulate morphology, easily accessible by electrolytes (Figure 5c,d). Using this structure as electrodes, the demonstrated cells showed cutoff frequency of ~ 40, and 80 Hz, depending on the material loading.[124]

MnO_2 has been well studied for pseudocapacitors, but it is highly insulating. rGO/MnO_2/Ag-NW hybrid films were investigated to enhance the conductivity (Figure 5e). With the interdigitated planar electrode configuration, the fabricated cells exhibited a large cutoff frequency between 1.3 to 6.3 kHz, and 120 Hz phase angles between −70° to −80° depending on the material loading.[125] Yan's group[88] reported graphene quantum dots (GQDs)//MnO_2 asymmetric microEC in the Na_2SO_4 electrolyte that exhibited high rate capability (1000 V s^{-1}) and high-frequency response (cutoff > 10 kHz) , but the phase angle is less than −70°, even at very low frequency (0.1 Hz). The areal capacitance was also small. The same group[126] further reported a similar structure, but using ionic liquid ionogel as solid electrolyte (Figure 5f). It exhibited excellent rate capability with the scan rate up to 2000 V s^{-1}, and a cutoff frequency as high as 4.8 kHz. However, the phase angle was only ~ −70° at low frequencies. The frequency response

of electrochemically active MnO_2 based EC is extraordinary, but the areal capacitance is low (~ 0.1 mF cm^{-2}), less than that of EDLCs. Their smaller phase angle, even at low frequency, suggests a larger ESR.

Transition metal dichalcogenides are also a group of pseudocapacitive materials. These are 2D sheet like materials providing large accessible surface area and interestingly, some of these show metallic phases with exceptionally low resistance.[133] Metallic VS_2,[134] MoS_2[135] and WS_2[136] have been studied as supercapacitor electrodes. Bissett *et al.* demonstrated dichalcogenides based supercapacitors with frequency responses in several kHz range.[137] These 2D nanostructured materials are highly promising in minimizing the typical sluggishness of pseudocapacitive materials, especially if combined with a conductive framework,[129,130] hence hold strong potential for compact high-frequency supercapacitors.

Conducting polymer-based redox micro-EC with good frequency response was also reported (Figure 5g,h).[127,138] Ti/Au metal stack covered by PEDOT electrodes was prepared by electrodeposition with an open porous structure. Such porous PEDOT facilitated ion transport for better rate capability. A phase angle of −80.5° at 120 Hz with a cell capacitance of 0.15 mF cm^{-2}, or a phase angle of −60° at 120 Hz with a cell capacitance of 1.3 mF cm^{-2} were measured, depending on the amount of material used. A cutoff frequency of ~ 1 kHz was confirmed. The large capacitance was attributed to the formation of double layers and pseudocapacitance from fast redox events such as doping/de-doping processes at the surface of conducting PEDOT polymer. The same group further compared PEDOT, polypyrrole (PPY), and polyaniline (PANI) as the active electrode material, with PEDOT giving the best high frequency response.

The most exciting results came from PEDOT:PSS as a precursor to produce the electrode material for kHz ECs with a large capacitance, which offers the opportunity to replace carbonaceous materials as an active electrode material. Highly conductive material from PEDOT:PSS, with a conductivity of 1400 S cm^{-1} was reported through sulfuric etching to break the binding between PEDOT and PSS.[139] On this basis, Shi's group[14] reported using sulfuric acid treated PEDOT:PSS as conductive polymer for kHz EC electrodes (Figure 5i-l). PEDOT:PSS films were coated on highly conductive graphite foil with a cellulose paper as a sacrificial template. Sulfuric acid treatment was applied to remove the cellulose fibers and partially etch away the insulating PSS component to obtain the porous and conductive structure. Depending on the film thickness (90 to 600 nm), the impedance phase angle at 120 Hz varied from −85.7° to −78.9°, and the relaxation time constant from 0.15 ms to 1.50 ms, while cell area capacitance increased from 0.23 mF cm^{-2} to 2.43 mF cm^{-2}, more than one order of magnitude. The active-material based volumetric capacitance density increased from 12.78 F cm^{-3} to 20.22 F cm^{-3}. The performances of these electrodes are superior, and the reported electrode preparation method is simple and scalable.

These high-rate results, from those materials that have been traditionally considered as electrochemically active and hence very slow, are unexpected. The studies along this line may find alternative materials other than carbon, for the ultimate goal of kHz ECs.

Table I. Representative results of kHz ECs, including electrode active material and electrolyte used, the active material thickness (t_a), the electrode (including active and inactive materials) thickness (t), cutoff frequency f_0, 120 Hz phase ($-\Phi_{120}$), RC constant (τ_{120}), single-electrode areal capacitance (C_{A120}), single-electrode active material volumetric capacitance density (C_{V120a}) and active-inactive material volumetric capacitance density (C_{v120}), and the maximum voltage window (V_{max}). Those in Refs. 67 and 127 are based on a planar microsupercapacitor structure, and others are based on a sandwich structure.

Ref.	Electrode material	Electrolyte	t_a (μm)	t (μm)	f_0 (kHz)	$-\Phi_{120}$ (°)	τ_{120} (ms)	C_{A120} (mF cm^{-2})	C_{V120a} (F cm^{-3})	C_{V120} (F cm^{-3})	V_{max} (V)
1	VOG	KOH	0.6	75.6	15	82	0.20	0.175	2.917	0.023	1
8	ErGO	KOH	20	220	4.2	84	1.35	0.566	0.283	0.026	1
9	VOG	KOH	2	77	6.3	85		0.53	2.65	0.069	1
11	EOG	KOH	–	200	4.03	82	0.248	0.72	–	0.036	1
12	EOG	KOH	–	10	12	83	0.110	0.6	–	0.6	1
			–	30	5.6	83		1.5	–	0.5	1
13	NHG	KOH	2		1.2	81.2	0.203	0.956	4.78		1
14	AT-PEDOT:PSS	H_2SO_4	0.09	16.09	6.56	85.7	0.099	0.460	51.11	0.286	1
			0.24	16.24	2.885	85.6	0.101	1.322	55.08	0.814	1
			0.39	16.39	1.178	82.2	0.178	3.342	85.69	2.039	1
15	SWCNT	$TEABF_4$	0.30	20.34	1.995	82.2	0.501	0.564	18.80	0.277	2.5
17	CNT	H_2SO_4	0.23		1.425	81	0.199	1.202	52.30		1
18	GOMC/CNT	$TEABF_4$	0.68		1.0	80.3		1.118	16.44		2.5
67	G/CNT	H_2SO_4/PVA	10		1.343	81.5	0.195	0.46	0.46		1
127	PEDOT	H_2SO_4/PVA	0.1		1.0	80.5	0.21	0.30	30		1

In Table I, a few representative results on kHz ECs with cutoff frequency $f_0 > 1$ kHz and 120 Hz phase angle value $-\Phi_{120} > 80^o$ are listed to show the state-of-the-art. As will be discussed in section 5 on high voltage kHz EC design based on multiple electrodes, the whole electrode capacitance density, including the volume of both active and inactive components in the electrode, is a critical parameter to design compact kHz ECs in competing to AECs. Therefore, we particularly list the single electrode areal and volumetric capacitance densities. In addition to a few freestanding electrode structures,[12] many of the reported electrodes consist of a very thin active layer deposited on a thick substrate, resulting a limited

volumetric capacitance density. However, our recent results (not published yet) and the data in Ref. 14 suggest that a 120 Hz volumetric capacitance density (C_{V120}) of a few F cm^{-3} is achievable.

5. Higher Voltage kHz EC Design

Electrolytic capacitors have rating voltage from a few volts up to several hundred volts, depending on the dielectric layer thickness. On the other hand, ECs are intrinsically low voltage devices, limited by the electrolyte decomposition potential. Of the three primary classes of electrolyte used, aqueous electrolyte cells have higher frequency performance but with a voltage window up to ~ 1 V; Organic electrolytes, typically based on acetonitrile or cyclic carbonates, have a high voltage window up to ~ 3.5 V but with a slightly lower cutoff frequency due to lower ionic conductivity;[140,141] Ionic liquids have a potential window up to ~ 5 V but with a lower ionic conductivity.[142-144] To obtain a high voltage rating, the kHz EC device structure would adopt a bipolar design through multi-cell connection in series. In term of voltage rating and device size, ionic liquids as electrolyte have a profound advantage, but the large electrolyte resistance prevents their application for room temperature kHz ECs. On the other hand, ionic liquids have high decomposition temperatures (well exceeding 100 ^{o}C)[145] and their resistance diminishes at higher temperatures,[10] and therefore, they might be used for high temperature kHz ECs. This is particularly true considering that some AEC filtering capacitors are rated for continuous operation at 125 ^{o}C for large current ripple filtering, while aqueous ECs are rated to an upper limit of 70 ^{o}C.

The frequency response from most reported electrode materials is tested in a coin cell assembly with a sandwich-type structure, where a porous separator is sandwiched by two electrodes. For high frequency response, most reported electrodes have a thin active material thickness of ~ 1 μm or less deposited on a thick current collector, while the separator has a thickness of ~ 10–30 μm. Since the volumetric capacitance is inversely proportional to the square of the number of cells in series, multi-cells based on such electrode structures in sandwich-type configuration would offer no volumetric advantages when comparing to commercially available AECs under the same voltage rating.

Miller *et al.*[10] discussed in detail the device structure design for high voltage operation. It was argued that for thin active material, planar-type cell structure with interdigitated electrodes should be considered. Planar-type cells are commonly fabricated to investigate the so-called "micro-ECs" targeting at on-chip micro-power sources.[146-150] In many of these reports, the prefix of "micro-" was used, which simply referred to a thin-film applied as the electrode active material. Such planar cells, if enough footprint is available, can have a large capacitance.

Three approaches: photolithography, laser ablation, and in-situ synthesis have been widely reported for planar cell fabrication. In the first method, metallic current collector pattern, in an interdigitated format

is first defined through photolithography and metallization. Then the active electrode material is deposited only on the metal pattern via inkjet printing, screen printing or electrophoretic deposition, thus forming the interdigitated electrode.[82,151,152] In the second approach, current collector layer and active material layer are uniformly deposited on an insulating substrate. Then laser ablation is conducted to cut through the active material and current collector, thus forming the micro-scale separation between the two interdigitated electrodes.[153] Technologies based on in-situ synthesis of the active material[154-159] include different methods such as laser irradiation-induced conversion, chemical conversion, or electrolytic deposition during fabrication.

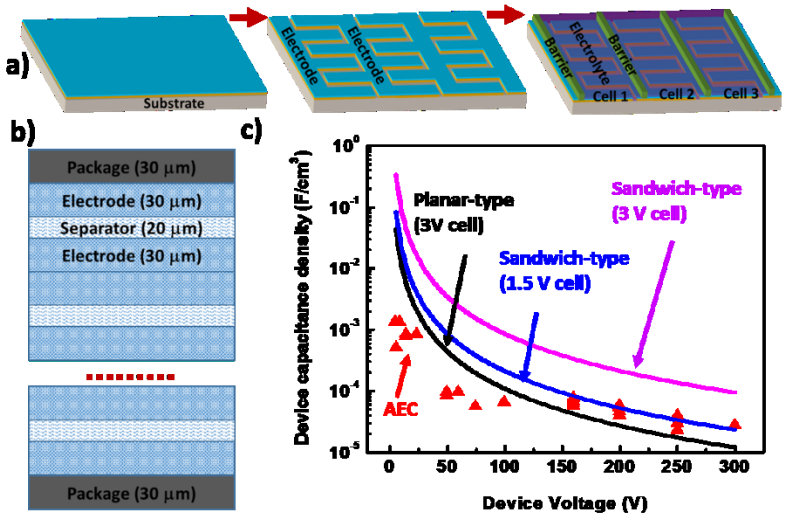

Figure 6. (a) Schematic illustrating major steps to produce integrated planar-type multi-cell in series for high voltage operation. (b) Schematic of sandwich-type multi-cell configuration. (c) Prediction of the capacity density of high-voltage ECs at different operation voltages, in comparison to commercial AECs. Adapted from Ref. 10 for (c), Copyright 2015, The Electrochemical Society.

Two approaches[10] for interconnecting planar cells to create high-voltage kHz ECs were proposed. The first approach involves stacking planar cells followed by interconnecting them on opposite edges in an accordion-like fashion. The second approach (Figure 6a) is to serially integrate multiple cells monolithically on the same substrate, in a fashion widely adopted for the manufacture of thin-film solar cell modules. Here gaps are cut between neighboring cells, and cells are individually covered with an electrolyte, making sure that each electrolyte band does not touch its neighbors through a barrier. The planar design, particularly the monolithic multiple cell integration approach offers significant volumetric advantages when the ultrathin film is used as the electrode material. Assuming each cell with a rating of

V_0, capacitance C_0, and ESR R_0, the serial connection of N cells using either approach yields a multi-cell capacitor with a rating of voltage NV_0, capacitance C_0/N, and ESR of NR_0. Therefore the multi-cell high-voltage capacitor has a frequency response nearly identical to that of a single cell. Since the volume proportionally increases by N folds, the capacitance density is inversely proportional to the square of rating voltage. Using the planar design in Figure 6a and their preliminary data, Miller *et al.*[10] provided informative predicting on the size advantage of future kHz ECs over AECs by assuming V_0 = 3.0 V, C_0 = 2.5 mF cm^{-2} and 50 μm total thickness. The predicted volumetric capacitance is 1.08/V^2 (F cm^{-3}) where V is the voltage rating. This equation is plotted in Figure 6c along with commercial AEC values. KHz ECs, based on the above parameter used, have volumetric advantages over AEC for voltages below ~100 V.

In the above planar design, ultrathin active material grown on a much thick current collector was assumed and correspondingly planar multi-cell design is a better approach. This design, however demands considerable footprint, and is not the best design when considering minimization of circuit board. In our work,[12] 30 μm thick freestanding electrodes were reported with an electrode capacitance density of 0.5 F cm^{-3} for the whole volume of electrode. Our recent work suggests that this value can be further improved by several folds. For such electrodes, the traditional sandwich-type structure is a better choice than the planar design in terms of fabrication cost, capacitance density, and footprint needed. To estimate the sandwich-type multi-cell high-voltage capacitor size, we assume 30 μm thick freestanding electrodes with an electrode capacitance density of 5 F cm^{-3}, and two operating voltage of 1.5 V and 3 V. We further assume a separator thickness of 20 μm, and a package thickness of 30 μm, where N-cells are stacked, and interconnected as schematically shown in Figure 6b. When N is large, the package thickness becomes negligible and the capacitor has a capacitance density of 2.1/V^2 or 8.5/V^2 (F cm^{-3}), depending on single cell voltage (1.5 V vs. 3 V). These are also plotted in Figure 6c. Volumetric advantages of kHz ECs over AECs are available for the whole voltage range up to 250 V, if a single cell runs at 3V. When an individual cell has a voltage of 1.5 V, then a multi-cell EC has volumetric merit up to a voltage ~ 150 V.

Since one of the main purposes to develop kHz EC is to have a smaller size in replacing bulky AEC, the choice of multi-cell configuration, sandwich-type or planar-type, mainly depends on the obtained volumetric capacitance for a given rating voltage. Based on the above predictions, we conclude that when an active material layer is ultrathin in micrometer scale, the planar-type cell structure should be adopted, while the traditional sandwich-type cell structure is still a better design, if the active material layer has a thickness of tens of micrometers.

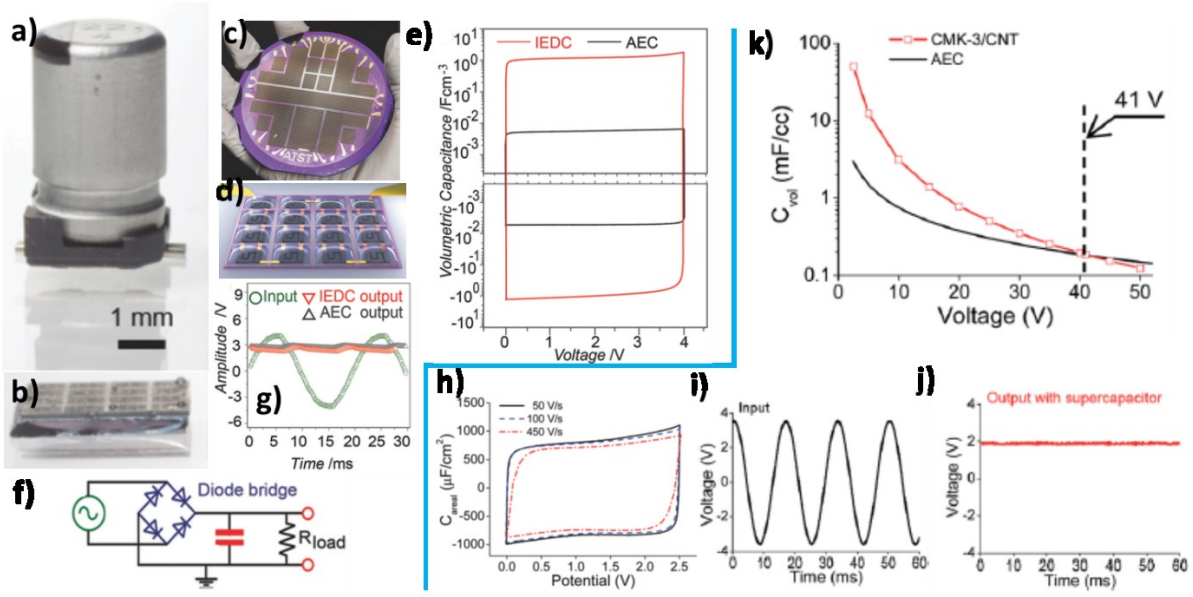

Figure 7. Optical photograph of a commercial AEC as a reference in (a), and the integrated planar EC in (b) with a volume reduction by more than 800 times. (c) Optical photograph of a wafer based integrated planar ECs. (d) Schematic of 16 integrated cells as one device. (e) CV scan indicating a capacitance density more than 800 times larger than the AEC reference. Using the filtering circuit in (f), the DC output from the integrated planar EC is comparable to that from the AEC. For a sandwich-type single cell tested for AC filtering: (h) CV curve of the cell, (i) the input voltage waveform of 60 Hz with V_p=±3.56 V, and (j) the output DC curve. (k) This specific CMK-3/CNT electrode based EC has a smaller size than AEC up to a voltage of 41 V. Reproduced with permission from Ref. 160 for (a-g), Copyright 2015, John Wiley and Sons; Ref. 18 for (h-k), Copyright 2016, Royal Society of Chemistry.

Toward preliminary demonstration using planar-type ECs as filtering capacitors, in substitute of bulky AEC, Laszczyk *et al.* reported their exciting work (Figure 7a-g).[160] A commercial AEC (Panasonic, 4 V, 22 μF) was used as a reference. Integrated planar cells were fabricated using photolithography with CNT film as an electrode material, and an epoxy (SU8) as an inter-cell barrier. Each individual cell was filled with aqueous electrolyte using a microinkjet. Sixteen cells, arranged as four in series banks of four parallel-connected cells, are integrated with 4 V operation voltage. Similar capacitance, relaxation time constant, and ripple filtering capability as the AEC was demonstrated by such an integrated device when tested in a filtering circuit, but with a much larger (> 800 folds) capacitance density. This demonstration is encouraging, but we cautiously point out the low frequency response of the device in this proof-concept

demonstration. Better electrode material structures, as reviewed in this article should be adopted, particularly for devices with a large capacitance, and for efficient filtering with less heat generation.

Kim's group[18] demonstrated CMK-3/CNTs based sandwich-type single cell for filtering application (Figure 7h-k). With $TEABF_4$ based organic electrolyte, the cell ran up to 2.5 V with a 120 Hz phase angle of ~ –80° and a capacitance of 0.56 mF cm^{-2}. Since the demonstrated cell has a volumetric capacitance of 50.2 mF cm^{-3}, it was further estimated that up to ~ 41 V such electrode based ECs have a more compact size than the commercial AECs.

The results from these preliminary testing for practical filtering applications, based on both planar-type and sandwich-type configurations, are very exciting, encouraging us in further developing compact kHz ECs for filtering and other potential applications.

6. Conclusion and Outlook

Since the first demonstration of kHz ECs in 2010 that had the potential to replace electrolytic capacitors, intensive interests have been drawn that result in dramatic progress in this exciting area. The areal and volumetric capacitance density of kHz ECs at 120 Hz have been increased by more than ten folds to 2.4 mF cm^{-2}, and 20 F cm^{-3}, respectively. In addition to VOG and EOG, several other electrode structures, both carbon based and non-carbon based, have also been proved suitable for kHz ECs. rGO gel, holy rGO film, vertically aligned CNT, ultrathin CNT film, highly conductive, and porous PEDOT:PSS films, among others, are particularly promising. In term of electrolyte and cell voltage, besides the commonly used aqueous electrolytes that facilitate high frequency response but with a low operation voltage, gel-based solid state electrolytes, organic electrolytes, and liquid ion electrolytes were also reported capable of response in the kHz frequency scope, particularly single cells running at 3V have been reported. Furthermore, as proof of concept, using such kHz ECs as filtering capacitor in low voltage AC/DC converters has been successfully demonstrated with filtering capability comparable to bulky electrolytic capacitors. In term of higher voltage kHz EC architectural design, planar-type structure, and sandwich structure have been analyzed. It is believed that with further improvement of capacitance density of nanostructured electrodes, and the single cell voltage up to 100 V or even 200 V, the kHz ECs could offer dramatic volumetric capacitance advantage over electrolytic capacitors. These progresses in the past several years declare the bright future of kHz EC, as a circuit element, for broad applications in power systems and power electronics, in contrast to the traditional applications of slow ECs as energy storage.

However, to realize such a vision into a reality, strong efforts are still required, and we believe the following particular issues should be further addressed.

1) 2D vs. 3D electrodes

As the guidelines in Section 2 suggested, to minimize porous effect for high frequency response, thin-film electrode is necessary, as has been confirmed by the different sub-μm thin-film structures reviewed in this paper. As analyzed in Section 5, such an electrode becomes problematic for building higher voltage multi-cells, when footprint is a major design parameter. For a given footprint, to have more active material loading, and simultaneously maintaining the sub-μm thickness, the commonly used 2D planar substrate (current collector) must extend into the 3rd dimension with a 3D configuration. The 3D current collector must have large pores at the scale of tens of micrometers, allowing sub-μm films deposited along the pore surface and providing rapid electrolyte transport paths. Promising results have been achieved along this direction,[12] but areal capacitance should be improved by another order of magnitude.

2) Quantum capacitance and DLC

The concept of quantum capacitance was introduced in 1988 to explain the impact of a limited density of states in 2-D electron gas, when used as "electrode", on the achievable capacitance.[161] The quantum capacitance of single and double layered graphene was later measured, and in the plot versus gate potential, it has a symmetric V-shape, and a minimum is located at the Dirac point, agreeing with the theoretical model of graphene.[162] Since massless Dirac fermions were also observed in graphite,[163] which coexist with quasiparticles with finite effective mass, quantum capacitance should also exist in graphite electrode. In the early 1970s, Randin et al.[40,164,165] had reported a similar phenomenon when studying differential capacitance in graphite based electrodes, and was explained at that time by a charge depletion layer in graphite, or a space charge capacitance, which resulted in a reduction of the total capacitance. In the community of ECs, particularly kHz ECs, the quantum capacitance effect has not caught enough attention. From a practical point of view, this might be understood that the so-called electric double layer effect nowadays in fact, include many different other effects, with a value of 5–20 μF/cm^2 generally reported.[26,166] Due to voltage dependent reorientation of solvent molecules in the dipole layer and other factors, any change of the double layer charge dQ depends on the already existing potential, therefore, differential capacitance has been reported, which can be easily measured using a constant charge/discharge current. This differential capacitance, generally exhibiting a V- or U-shape, was traditionally explained by the separated space charge densities established at the interface: electron deficiency or accumulation at the electrode surface and solvated cations or anions in the solution. With the concept of quantum capacitance, we should re-examine this phenomenon. On the other hand, from the point of view of developing kHz EC electrodes with large capacitance density, how to minimize the

quantum capacitance effect which otherwise reduces the total capacitance, particularly for the VOG and EOG based electrodes, should draw enough attention.[167]

3) Electrochemically active material and pseudocapacitance

Initial studies have suggested that metallic oxides and nitrides might also be applied for fast ECs. Since a cutoff frequency of more than 100 Hz has been reported,[123] it is intriguing to ask the question: can it further be improved into the kHz frequency? On the other hand, conductive polymer based, rGO/MnO_2/Ag-NW based, and GQDs//MnO_2 asymmetric cells, all have entered into the kHz frequency range, and they were claimed to be pseudocapacitors.[125-127] Whether the redox reactions can occur in such a flash rate, or the observed high-frequency capacitance simply comes from double layer effects needs to be further investigated.

4) Electrode materials other than carbon

The unprecedented results from the acid-treated PEDOT:PSS,[14] particularly the much larger high-frequency capacitance density than those of the variety of carbonaceous materials, suggest materials other than carbon should be another research direction towards the goal of kHz ECs. The success of PEDOT:PSS lies in two aspects: coating on a sacrificial scaffold to introduce macro-scale pore structure, and etching away the insulating PSS component to obtain more porous and higher conductive structure. Other materials with intrinsic high conductivity may also be engineered with porous structure along this line for kHz ECs.

In addition to the studies of electrode materials and nanostructures, we also emphasize that the electrolyte plays critical roles in determining the frequency response, the voltage rating, the temperature rating,[168] and the device volume of the EC. The aqueous electrolyte, with their higher ionic conductivity and smaller solvated ion size, contribute to higher frequency response. However, their lower operation voltage and lower thermal stability put severe limitations on the voltage and ripple current handling capability of the filtering EC. Therefore, enough attentions should also be paid in this aspect for developing practical devices.

Currently, the research efforts in kHz ECs centers on current ripple filtering in AC/DC conversion. It is expected that with the progress in both frequency response and capacitance density, these devices may also be capable of other functions in power electronics traditionally accomplished by the electrolytic capacitors, and find new applications such as integration onto Si IC chips, MEMS chips, and others as high-density on-chip capacitors.

Acknowledgements: This work is supported by National Science Foundation (1611060). Z.F also acknowledges the support from GLEAMM. We greatly appreciate that Dr. John R. Miller from JME, Inc. & Case Western Reserve University reviewed the manuscript and offered his encouragement and critical comments on improving the manuscript quality.

References:

(1) Miller, J. R.; Outlaw, R. A.; Holloway, B. C. Graphene double-layer capacitor with ac line-filtering performance. *Science* **2010**, *329*, 1637-1639.

(2) Gallay, R.; Gualous, H.: Industrial production of double-layer capacitors. In *Carbons for electrochemical energy storage and conversion systems*; CRC Press, 2009; pp 429-467.

(3) Toupin, M.; Bélanger, D.; Hill, I. R.; Quinn, D. Performance of experimental carbon blacks in aqueous supercapacitors. *Journal of power sources* **2005**, *140*, 203-210.

(4) Miller, J. R. Introduction to electrochemical capacitor technology. *IEEE Electrical Insulation Magazine* **2010**, *26*, 40-47.

(5) Both, J. The modern era of aluminum electrolytic capacitors. *IEEE Electrical Insulation Magazine* **2015**, *31*, 24-34.

(6) Both, J. Electrolytic capacitors from the postwar period to the present. *IEEE Electrical Insulation Magazine* **2016**, *32*, 8-26.

(7) Fan, F.-R.; Tian, Z.-Q.; Wang, Z. L. Flexible triboelectric generator. *Nano Energy* **2012**, *1*, 328-334.

(8) Sheng, K.; Sun, Y.; Li, C.; Yuan, W.; Shi, G. Ultrahigh-rate supercapacitors based on eletrochemically reduced graphene oxide for ac line-filtering. *Sci Rep* **2012**, *2*, 247.

(9) Cai, M.; Outlaw, R. A.; Quinlan, R. A.; Premathilake, D.; Butler, S. M.; Miller, J. R. Fast Response, vertically oriented graphene nanosheet electric double layer capacitors synthesized from C(2)H(2). *ACS Nano* **2014**, *8*, 5873-5882.

(10) Miller, J. R.; Outlaw, R. A. Vertically-oriented graphene electric double layer capacitor designs. *Journal of The Electrochemical Society* **2015**, *162*, A5077-A5082.

(11) Ren, G.; Pan, X.; Bayne, S.; Fan, Z. Kilohertz ultrafast electrochemical supercapacitors based on perpendicularly-oriented graphene grown inside of nickel foam. *Carbon* **2014**, *71*, 94-101.

(12) Ren, G.; Li, S.; Fan, Z.-X.; Hoque, M. N. F.; Fan, Z. Ultrahigh-rate supercapacitors with large capacitance based on edge oriented graphene coated carbonized cellulous paper as flexible freestanding electrodes. *Journal of Power Sources* **2016**, *325*, 152-160.

(13) Zhou, Q.; Zhang, M.; Chen, J.; Hong, J. D.; Shi, G. Nitrogen-Doped Holey Graphene Film-Based Ultrafast Electrochemical Capacitors. *ACS Appl Mater Interfaces* **2016**, *8*, 20741-20747.

(14) Zhang, M.; Zhou, Q.; Chen, J.; Yu, X.; Huang, L.; Li, Y.; Li, C.; Shi, G. An ultrahigh-rate electrochemical capacitor based on solution-processed highly conductive PEDOT: PSS films for AC line-filtering. *Energy & Environmental Science* **2016**, *9*, 2005-2010.

(15) Yoo, Y.; Kim, S.; Kim, B.; Kim, W. 2.5 V compact supercapacitors based on ultrathin carbon nanotube films for AC line filtering. *J. Mater. Chem. A* **2015**, *3*, 11801-11806.

(16) Kang, Y. J.; Yoo, Y.; Kim, W. 3-V Solid-State Flexible Supercapacitors with Ionic-Liquid-Based Polymer Gel Electrolyte for AC Line Filtering. *ACS Appl Mater Interfaces* **2016**, *8*, 13909-13917.

(17) Rangom, Y.; Tang, X. S.; Nazar, L. F. Carbon Nanotube-Based Supercapacitors with Excellent ac Line Filtering and Rate Capability via Improved Interfacial Impedance. *ACS Nano* **2015**, *9*, 7248-7255.

(18) Yoo, Y.; Kim, M. S.; Kim, J. K.; Kim, Y. S.; Kim, W. Fast-response supercapacitors with graphitic ordered mesoporous carbons and carbon nanotubes for AC line filtering. *Journal of Materials Chemistry A* **2016**, *4*, 5062-5068.

(19) Taberna, P. L.; Simon, P.; Fauvarque, J. F. Electrochemical Characteristics and Impedance Spectroscopy Studies of Carbon-Carbon Supercapacitors. *Journal of The Electrochemical Society* **2003**, *150*, A292.

(20) Kötz, R.; Carlen, M. Principles and applications of electrochemical capacitors. *Electrochimica acta* **2000**, *45*, 2483-2498.

(21) Gamby, J.; Taberna, P.; Simon, P.; Fauvarque, J.; Chesneau, M. Studies and characterisations of various activated carbons used for carbon/carbon supercapacitors. *Journal of power sources* **2001**, *101*, 109-116.

(22) Lin, R.; Taberna, P.-L.; Chmiola, J.; Guay, D.; Gogotsi, Y.; Simon, P. Microelectrode study of pore size, ion size, and solvent effects on the charge/discharge behavior of microporous carbons for electrical double-layer capacitors. *Journal of the Electrochemical Society* **2009**, *156*, A7-A12.

(23) Li, X.; Rong, J.; Wei, B. Electrochemical behavior of single-walled carbon nanotube supercapacitors under compressive stress. *ACS nano* **2010**, *4*, 6039-6049.

(24) De Levie, R. On porous electrodes in electrolyte solutions: I. Capacitance effects. *Electrochimica Acta* **1963**, *8*, 751-780.

(25) Ghosh, A.; Le, V. T.; Bae, J. J.; Lee, Y. H. TLM-PSD model for optimization of energy and power density of vertically aligned carbon nanotube supercapacitor. *Scientific reports* **2013**, *3*, 2939.

(26) Zhang, L. L.; Zhao, X. Carbon-based materials as supercapacitor electrodes. *Chemical Society Reviews* **2009**, *38*, 2520-2531.

(27) Niu, C.; Sichel, E. K.; Hoch, R.; Moy, D.; Tennent, H. High power electrochemical capacitors based on carbon nanotube electrodes. *Applied Physics Letters* **1997**, *70*, 1480-1482.

(28) An, K. H.; Kim, W. S.; Park, Y. S.; Moon, J.-M.; Bae, D. J.; Lim, S. C.; Lee, Y. S.; Lee, Y. H. Electrochemical properties of high-power supercapacitors using single-walled carbon nanotube electrodes. *Advanced functional materials* **2001**, *11*, 387-392.

(29) Yoon, B.-J.; Jeong, S.-H.; Lee, K.-H.; Kim, H. S.; Park, C. G.; Han, J. H. Electrical properties of electrical double layer capacitors with integrated carbon nanotube electrodes. *Chemical Physics Letters* **2004**, *388*, 170-174.

(30) Du, C.; Pan, N. Supercapacitors using carbon nanotubes films by electrophoretic deposition. *Journal of Power Sources* **2006**, *160*, 1487-1494.

(31) Du, C.; Pan, N. High power density supercapacitor electrodes of carbon nanotube films by electrophoretic deposition. *Nanotechnology* **2006**, *17*, 5314-5318.

(32) Miller, J. R.; Outlaw, R.; Holloway, B. Graphene electric double layer capacitor with ultra-high-power performance. *Electrochimica Acta* **2011**, *56*, 10443-10449.

(33) Malesevic, A.; Vitchev, R.; Schouteden, K.; Volodin, A.; Zhang, L.; Van Tendeloo, G.; Vanhulsel, A.; Van Haesendonck, C. Synthesis of few-layer graphene via microwave plasma-enhanced chemical vapour deposition. *Nanotechnology* **2008**, *19*, 305604.

(34) Chen, J.; Bo, Z.; Lu, G. Vertically-Oriented Graphene. *Springer International Publishing Switzerland, DOI* **2015**, *10*, 978-973.

(35) Hiramatsu, M.; Hori, M.: *Carbon nanowalls: synthesis and emerging applications*; Springer Science & Business Media, 2010.

(36) Ren, G.; Hoque, M. N. F.; Liu, J.; Warzywoda, J.; Fan, Z. Perpendicular edge oriented graphene foam supporting orthogonal TiO 2 (B) nanosheets as freestanding electrode for lithium ion battery. *Nano Energy* **2016**, *21*, 162-171.

(37) Ren, G.; Hoque, M. N. F.; Pan, X.; Warzywoda, J.; Fan, Z. Vertically aligned VO 2 (B) nanobelt forest and its three-dimensional structure on oriented graphene for energy storage. *Journal of Materials Chemistry A* **2015**, *3*, 10787-10794.

(38) McCreery, R. L. Advanced carbon electrode materials for molecular electrochemistry. *Chem. Rev* **2008**, *108*, 2646-2687.

(39) Pan, X.; Zhu, K.; Ren, G.; Islam, N.; Warzywoda, J.; Fan, Z. Electrocatalytic properties of a vertically oriented graphene film and its application as a catalytic counter electrode for dye-sensitized solar cells. *Journal of Materials Chemistry A* **2014**, *2*, 12746-12753.

(40) Randin, J.-P.; Yeager, E. Differential capacitance study on the edge orientation of pyrolytic graphite and glassy carbon electrodes. *Journal of Electroanalytical Chemistry and Interfacial Electrochemistry* **1975**, *58*, 313-322.

(41) Cai, M.; Outlaw, R. A.; Butler, S. M.; Miller, J. R. A high density of vertically-oriented graphenes for use in electric double layer capacitors. *Carbon* **2012**, *50*, 5481-5488.

(42) Bo, Z.; Wen, Z.; Kim, H.; Lu, G.; Yu, K.; Chen, J. One-step fabrication and capacitive behavior of electrochemical double layer capacitor electrodes using vertically-oriented graphene directly grown on metal. *Carbon* **2012**, *50*, 4379-4387.

(43) Premathilake, D.; Outlaw, R. A.; Parler, S. G.; Butler, S. M.; Miller, J. R. Electric double layer capacitors for ac filtering made from vertically oriented graphene nanosheets on aluminum. *Carbon* **2017**, *111*, 231-237.

(44) Quinlan, R. A.; Cai, M.; Outlaw, R. A.; Butler, S. M.; Miller, J. R.; Mansour, A. N. Investigation of defects generated in vertically oriented graphene. *Carbon* **2013**, *64*, 92-100.

(45) Shuai, X.; Bo, Z.; Kong, J.; Yan, J.; Cen, K. Wettability of vertically-oriented graphenes with different intersheet distances. *Rsc Adv* **2017**, *7*, 2667-2675.

(46) Yang, H.; Yang, J.; Bo, Z.; Zhang, S.; Yan, J.; Cen, K. Edge effects in vertically-oriented graphene based electric double-layer capacitors. *Journal of Power Sources* **2016**, *324*, 309-316.

(47) Bo, Z.; Yang, H.; Zhang, S.; Yang, J.; Yan, J.; Cen, K. Molecular Insights into Aqueous NaCl Electrolytes Confined within Vertically-oriented Graphenes. *Scientific reports* **2015**, *5*, 14652.

(48) Cao, X.; Shi, Y.; Shi, W.; Lu, G.; Huang, X.; Yan, Q.; Zhang, Q.; Zhang, H. Preparation of novel 3D graphene networks for supercapacitor applications. *Small* **2011**, *7*, 3163-3168.

(49) Huang, H.; Tang, Y.; Xu, L.; Tang, S.; Du, Y. Direct formation of reduced graphene oxide and 3D lightweight nickel network composite foam by hydrohalic acids and its application for high-performance supercapacitors. *ACS applied materials & interfaces* **2014**, *6*, 10248-10257.

(50) Qi, J. L.; Lin, J. H.; Wang, X.; Le Guo, J.; Xue, L. F.; Feng, J. C.; Fei, W.-D. Low resistance VFG-Microporous hybrid Al-based electrodes for supercapacitors. *Nano Energy* **2016**, *26*, 657-667.

(51) Ding, Y.; Zhang, Z.: *Nanoporous metals for advanced energy technologies*; Springer, 2016.

(52) Gao, H.; Li, J.; Miller, J. R.; Outlaw, R. A.; Butler, S.; Lian, K. Solid-state electric double layer capacitors for ac line-filtering. *Energy Storage Materials* **2016**, *4*, 66-70.

(53) Quan, B.; Meng, Y.; Li, L.; Yao, Z.; Liu, Z.; Wang, K.; Wei, Z.; Gu, C.; Li, J. Vertical few-layer Graphene/metalized Si-nanocone arrays as 3D Electrodes for Solid-State Supercapacitors with Large Areal Capacitance and Superior Rate Capability. *Applied Surface Science* **2017**.

(54) Yoon, Y.; Lee, K.; Kwon, S.; Seo, S.; Yoo, H.; Kim, S.; Shin, Y.; Park, Y.; Kim, D.; Choi, J. Y.; Lee, H. Vertical alignments of graphene sheets spatially and densely piled for fast ion diffusion in compact supercapacitors. *ACS Nano* **2014**, *8*, 4580-4590.

(55) Zhu, J.; Sakaushi, K.; Clavel, G.; Shalom, M.; Antonietti, M.; Fellinger, T.-P. A general salt-templating method to fabricate vertically aligned graphitic carbon nanosheets and their metal carbide hybrids for superior lithium ion batteries and water splitting. *J. Am. Chem. Soc* **2015**, *137*, 5480-5485.

(56) Zhang, L.; Shi, G. Q. Preparation of Highly Conductive Graphene Hydrogels for Fabricating Supercapacitors with High Rate Capability. *J Phys Chem C* **2011**, *115*, 17206-17212.

(57) Chen, Z.; Ren, W.; Gao, L.; Liu, B.; Pei, S.; Cheng, H.-M. Three-dimensional flexible and conductive interconnected graphene networks grown by chemical vapour deposition. *Nature materials* **2011**, *10*, 424-428.

(58) Chen, J.; Sheng, K.; Luo, P.; Li, C.; Shi, G. Graphene hydrogels deposited in nickel foams for high- rate electrochemical capacitors. *Adv Mater* **2012**, *24*, 4569-4573.

(59) Chou, T. C.; Huang, C. H.; Doong, R. A.; Hu, C. C. Architectural design of hierarchically ordered porous carbons for high-rate electrochemical capacitors. *Journal of Materials Chemistry A* **2013**, *1*, 2886-2895.

(60) Nathan-Walleser, T.; Lazar, I. M.; Fabritius, M.; Tolle, F. J.; Xia, Q.; Bruchmann, B.; Venkataraman, S. S.; Schwab, M. G.; Mulhaupt, R. 3D Micro-Extrusion of Graphene-based Active Electrodes: Towards High-Rate AC Line Filtering Performance Electrochemical Capacitors. *Advanced Functional Materials* **2014**, *24*, 4706-4716.

(61) Shao, Y.; El-Kady, M. F.; Lin, C. W.; Zhu, G.; Marsh, K. L.; Hwang, J. Y.; Zhang, Q.; Li, Y.; Wang, H.; Kaner, R. B. 3D Freeze-Casting of Cellular Graphene Films for Ultrahigh-Power-Density Supercapacitors. *Adv Mater* **2016**, *28*, 6719-6726.

(62) Chang, Y.; Han, G.; Fu, D.; Liu, F.; Li, M.; Li, Y.; Liu, C. Paper-like N-doped graphene films prepared by hydroxylamine diffusion induced assembly and their ultrahigh-rate capacitive properties. *Electrochimica Acta* **2014**, *115*, 461-470.

(63) Paton, K. R.; Varrla, E.; Backes, C.; Smith, R. J.; Khan, U.; O'Neill, A.; Boland, C.; Lotya, M.; Istrate, O. M.; King, P. Scalable production of large quantities of defect-free few-layer graphene by shear exfoliation in liquids. *Nature materials* **2014**, *13*, 624-630.

(64) Chen, X.; Dobson, J. F.; Raston, C. L. Vortex fluidic exfoliation of graphite and boron nitride. *Chemical Communications* **2012**, *48*, 3703-3705.

(65) Wu, Z. S.; Liu, Z.; Parvez, K.; Feng, X.; Mullen, K. Ultrathin Printable Graphene Supercapacitors with AC Line-Filtering Performance. *Adv Mater* **2015**, *27*, 3669-3675.

(66) Parvez, K.; Li, R.; Puniredd, S. R.; Hernandez, Y.; Hinkel, F.; Wang, S.; Feng, X.; Müllen, K. Electrochemically exfoliated graphene as solution-processable, highly conductive electrodes for organic electronics. *ACS nano* **2013**, *7*, 3598-3606.

(67) Lin, J.; Zhang, C.; Yan, Z.; Zhu, Y.; Peng, Z.; Hauge, R. H.; Natelson, D.; Tour, J. M. 3-Dimensional graphene carbon nanotube carpet-based microsupercapacitors with high electrochemical performance. *Nano Lett* **2013**, *13*, 72-78.

(68) Schindall, J.; Kassakian, J.; Signorelli, R. In *Tilte*, San Diego, CA2007.

(69) Honda, Y.; Haramoto, T.; Takeshige, M.; Shiozaki, H.; Kitamura, T.; Ishikawa, M. Aligned MWCNT sheet electrodes prepared by transfer methodology providing high-power capacitor performance. *Electrochemical and Solid-State Letters* **2007**, *10*, A106-A110.

(70) Dörfler, S.; Felhösi, I.; Kek, I.; Marek, T.; Althues, H.; Kaskel, S.; Nyikos, L. Tailoring structural and electrochemical properties of vertical aligned carbon nanotubes on metal foil using scalable wet-chemical catalyst deposition. *Journal of Power Sources* **2012**, *208*, 426-433.

(71) Dörfler, S.; Felhösi, I.; Marek, T.; Thieme, S.; Althues, H.; Nyikos, L.; Kaskel, S. High power supercap electrodes based on vertical aligned carbon nanotubes on aluminum. *Journal of Power Sources* **2013**, *227*, 218-228.

(72) Wang, W.; Ozkan, M.; Ozkan, C. S. Ultrafast high energy supercapacitors based on pillared graphene nanostructures. *Journal of Materials Chemistry A* **2016**, *4*, 3356-3361.

(73) Kossyrev, P. Carbon black supercapacitors employing thin electrodes. *Journal of Power Sources* **2012**, *201*, 347-352.

(74) Joseph, J.; Paravannoor, A.; Nair, S. V.; Han, Z. J.; Ostrikov, K. K.; Balakrishnan, A. Supercapacitors based on camphor-derived meso/macroporous carbon sponge electrodes with ultrafast frequency response for ac line-filtering. *Journal of Materials Chemistry A* **2015**, *3*, 14105-14108.

(75) Paravannoor, A.; Nair, A. S.; Ranjusha, R.; Praveen, P.; Subramanian, K. R.; Sivakumar, N.; Nair, S. V.; Balakrishnan, A. Camphoric carbon- grafted Ni/NiO nanowire electrodes for high-performance energy- storage systems. *ChemPlusChem* **2013**, *78*, 1258-1265.

(76) Wei, H.; Wei, S.; Tian, W.; Zhu, D.; Liu, Y.; Yuan, L.; Li, X. Fabrication of thickness controllable free-standing sandwich-structured hybrid carbon film for high-rate and high-power supercapacitor. *Scientific reports* **2014**, *4*, 7050.

(77) Liu, Y.; Yuan, L.; Yue, Y.; Hu, M.; Wei, H. Fabrication of 3D foam-like hybrid carbon materials of porous carbon/graphene and its electrochemical performance. *Electrochimica Acta* **2016**, *196*, 153-161.

(78) Eftekhari, A.; Fan, Z. Ordered Mesoporous Carbon and Its Applications for Electrochemical Energy Storage and Conversion. *Materials Chemistry Frontiers* **2017**.

(79) Korenblit, Y.; Rose, M.; Kockrick, E.; Borchardt, L.; Kvit, A.; Kaskel, S.; Yushin, G. High-rate electrochemical capacitors based on ordered mesoporous silicon carbide-derived carbon. *Acs Nano* **2010**, *4*, 1337-1344.

(80) Liang, C.; Li, Z.; Dai, S. Mesoporous carbon materials: synthesis and modification. *Angewandte Chemie International Edition* **2008**, *47*, 3696-3717.

(81) Ma, T.-Y.; Liu, L.; Yuan, Z.-Y. Direct synthesis of ordered mesoporous carbons. *Chemical Society Reviews* **2013**, *42*, 3977-4003.

(82) Pech, D.; Brunet, M.; Taberna, P.-L.; Simon, P.; Fabre, N.; Mesnilgrente, F.; Conédéra, V.; Durou, H. Elaboration of a microstructured inkjet-printed carbon electrochemical capacitor. *Journal of Power Sources* **2010**, *195*, 1266-1269.

(83) Heon, M.; Lofland, S.; Applegate, J.; Nolte, R.; Cortes, E.; Hettinger, J. D.; Taberna, P.-L.; Simon, P.; Huang, P.; Brunet, M. Continuous carbide-derived carbon films with high volumetric capacitance. *Energy & Environmental Science* **2011**, *4*, 135-138.

(84) Pech, D.; Brunet, M.; Durou, H.; Huang, P.; Mochalin, V.; Gogotsi, Y.; Taberna, P.-L.; Simon, P. Ultrahigh-power micrometre-sized supercapacitors based on onion-like carbon. *Nature nanotechnology* **2010**, *5*, 651-654.

(85) Kaempgen, M.; Chan, C. K.; Ma, J.; Cui, Y.; Gruner, G. Printable thin film supercapacitors using single-walled carbon nanotubes. *Nano letters* **2009**, *9*, 1872-1876.

(86) Gao, W.; Singh, N.; Song, L.; Liu, Z.; Reddy, A. L. M.; Ci, L.; Vajtai, R.; Zhang, Q.; Wei, B.; Ajayan, P. M. Direct laser writing of micro-supercapacitors on hydrated graphite oxide films. *Nature Nanotechnology* **2011**, *6*, 496-500.

(87) Beidaghi, M.; Wang, C. Micro-Supercapacitors Based on Interdigital Electrodes of Reduced Graphene Oxide and Carbon Nanotube Composites with Ultrahigh Power Handling Performance. *Advanced Functional Materials* **2012**, *22*, 4501-4510.

(88) Liu, W. W.; Feng, Y. Q.; Yan, X. B.; Chen, J. T.; Xue, Q. J. Superior Micro-Supercapacitors Based on Graphene Quantum Dots. *Advanced Functional Materials* **2013**, *23*, 4111-4122.

(89) Wu, Z. S.; Parvez, K.; Feng, X.; Mullen, K. Graphene-based in-plane micro-supercapacitors with high power and energy densities. *Nat Commun* **2013**, *4*, 2487.

(90) Wu, Z.-S.; Parvez, K.; Feng, X.; Müllen, K. Photolithographic fabrication of high-performance all-solid-state graphene-based planar micro-supercapacitors with different interdigital fingers. *Journal of Materials Chemistry A* **2014**, *2*, 8288-8293.

(91) Kim, B. C.; Hong, J. Y.; Wallace, G. G.; Park, H. S. Recent progress in flexible electrochemical capacitors: electrode materials, device configuration, and functions. *Advanced Energy Materials* **2015**, *5*.

(92) Maiti, U. N.; Lim, J.; Lee, K. E.; Lee, W. J.; Kim, S. O. Three- dimensional shape engineered, interfacial gelation of reduced graphene oxide for high rate, large capacity supercapacitors. *Advanced materials* **2014**, *26*, 615-619.

(93) Shao, Q. G.; Tang, J.; Lin, Y. X.; Li, J.; Qin, F. X.; Zhang, K.; Yuan, J. S.; Qin, L. C. Ionic liquid modified graphene for supercapacitors with high rate capability. *Electrochimica Acta* **2015**, *176*, 1441-1446.

(94) Lee, K.; Song, H.; Lee, K. H.; Choi, S. H.; Jang, J. H.; Char, K.; Son, J. G. Nickel nanofoam/different phases of ordered mesoporous carbon composite electrodes for superior capacitive energy storage. *ACS applied materials & interfaces* **2016**, *8*, 22516-22525.

(95) Choi, B. G.; Yang, M.; Hong, W. H.; Choi, J. W.; Huh, Y. S. 3D macroporous graphene frameworks for supercapacitors with high energy and power densities. *ACS Nano* **2012**, *6*, 4020-4028.

(96) Huang, M.; Jiang, X.; Zhang, H.; Yin, H.; Li, X.; Ju, X. Bowl-like carbon sheet for high-rate electrochemical capacitor application. *Journal of Power Sources* **2014**, *272*, 1-7.

(97) Zhu, J.; Xu, Y.; Zhang, Y.; Feng, T.; Wang, J.; Mao, S.; Xiong, L. Porous and high electronic conductivity nitrogen-doped nano-sheet carbon derived from polypyrrole for high-power supercapacitors. *Carbon* **2016**, *107*, 638-645.

(98) Zhang, L. L.; Zhao, X.; Stoller, M. D.; Zhu, Y.; Ji, H.; Murali, S.; Wu, Y.; Perales, S.; Clevenger, B.; Ruoff, R. S. Highly conductive and porous activated reduced graphene oxide films for high-power supercapacitors. *Nano Lett* **2012**, *12*, 1806-1812.

(99) Zhang, L.; Zhang, F.; Yang, X.; Long, G.; Wu, Y.; Zhang, T.; Leng, K.; Huang, Y.; Ma, Y.; Yu, A.; Chen, Y. Porous 3D graphene-based bulk materials with exceptional high surface area and excellent conductivity for supercapacitors. *Sci Rep* **2013**, *3*, 1408.

(100) Zhang, J.; Yang, W.; Liu, J. Facile fabrication of supercapacitors with high rate capability using graphene/nickel foam electrode. *Electrochimica Acta* **2016**, *209*, 85-94.

(101) Yang, W.; Yang, W.; Ding, F.; Sang, L.; Ma, Z. P.; Shao, G. J. Template-free synthesis of ultrathin porous carbon shell with excellent conductivity for high-rate supercapacitors. *Carbon* **2017**, *111*, 419-427.

(102) Wang, L. X.; Wang, R. R.; Zhao, H. Y.; Liu, L.; Jia, D. Z. High rate performance porous carbon prepared from coal for supercapacitors. *Mater Lett* **2015**, *149*, 85-88.

(103) Jiang, L.; Yan, J. W.; Zhou, Y.; Hao, L. X.; Xue, R.; Jiang, L.; Yi, B. L. Activated carbon/graphene composites with high-rate performance as electrode materials for electrochemical capacitors. *J Solid State Electr* **2013**, *17*, 2949-2958.

(104) Jiang, L.; Yan, J. W.; Xue, R.; Sun, G. Q.; Yi, B. L. Partially graphitized ordered mesoporous carbons for high-rate supercapacitors. *J Solid State Electr* **2014**, *18*, 2175-2182.

(105) Chen, J.; Sheng, K. X.; Luo, P. H.; Li, C.; Shi, G. Q. Graphene Hydrogels Deposited in Nickel Foams for High-Rate Electrochemical Capacitors. *Advanced Materials* **2012**, *24*, 4569-4573.

(106) Peng, H.; Ma, G. F.; Sun, K. J.; Mu, J. J.; Zhou, X. Z.; Lei, Z. Q. A novel fabrication of nitrogen-containing carbon nanospheres with high rate capability as electrode materials for supercapacitors. *Rsc Advances* **2015**, *5*, 12034-12042.

(107) Yang, J.; Zhang, E.; Li, X.; Yu, Y.; Qu, J.; Yu, Z.-Z. Direct Reduction of Graphene Oxide by Ni Foam as a High-Capacitance Supercapacitor Electrode. *ACS Applied Materials & Interfaces* **2016**, *8*, 2297-2305.

(108) Zhao, X.; Tian, H.; Zhu, M.; Tian, K.; Wang, J. J.; Kang, F.; Outlaw, R. A. Carbon nanosheets as the electrode material in supercapacitors. *Journal of Power Sources* **2009**, *194*, 1208-1212.

(109) Huang, H.; Lei, C.; Luo, G.; Li, G.; Liang, X.; Tang, S.; Du, Y. UV-assisted reduction of graphene oxide on Ni foam as high performance electrode for supercapacitors. *Carbon* **2016**, *107*, 917-924.

(110) Pham, D. T.; Lee, T. H.; Luong, D. H.; Yao, F.; Ghosh, A.; Le, V. T.; Kim, T. H.; Li, B.; Chang, J.; Lee, Y. H. Carbon nanotube-bridged graphene 3D building blocks for ultrafast compact supercapacitors. *ACS Nano* **2015**, *9*, 2018-2027.

(111) Wang, C.; Liu, D.; Chen, S.; Sang, Y.; Haleem, Y. A.; Wu, C.; Xu, W.; Fang, Q.; Habib, M.; Cao, J.; Niu, Z.; Ajayan, P. M.; Song, L. All-Carbon Ultrafast Supercapacitor by Integrating Multidimensional Nanocarbons. *Small* **2016**, *12*, 5684–5691.

(112) Yun, X. L.; Wang, J.; Shen, L. F.; Dou, H.; Zhang, X. G. Three-dimensional graphene nanosheets/carbon nanotube paper as flexible electrodes for electrochemical capacitors. *Rsc Adv* **2015**, *5*, 22173-22177.

(113) Wilson, E.; Islam, M. F. Ultracompressible, high-rate supercapacitors from graphene-coated carbon nanotube aerogels. *ACS Appl Mater Interfaces* **2015**, *7*, 5612-5618.

(114) Pan, Z. Z.; Dong, L.; Lv, W.; Zheng, D.; Li, Z.; Luo, C.; Zheng, C.; Yang, Q. H.; Kang, F. A hollow spherical carbon derived from the spray drying of corncob lignin for high rate-performance supercapacitors. *Chem Asian J* **2017**, *12*, 503–506.

(115) Cheng, P.; Li, T.; Yu, H.; Zhi, L.; Liu, Z.; Lei, Z. Biomass-Derived Carbon Fiber Aerogel as a Binder-Free Electrode for High-Rate Supercapacitors. *The Journal of Physical Chemistry C* **2016**, *120*, 2079-2086.

(116) Wang, H.; Xu, Z.; Kohandehghan, A.; Li, Z.; Cui, K.; Tan, X.; Stephenson, T. J.; King'ondu, C. K.; Holt, C. M.; Olsen, B. C.; Tak, J. K.; Harfield, D.; Anyia, A. O.; Mitlin, D. Interconnected carbon nanosheets derived from hemp for ultrafast supercapacitors with high energy. *ACS Nano* **2013**, *7*, 5131-5141.

(117) Wang, C.; Liu, D.; Chen, S.; Sang, Y.; Haleem, Y. A.; Wu, C.; Xu, W.; Fang, Q.; Habib, M.; Cao, J. All- Carbon Ultrafast Supercapacitor by Integrating Multidimensional Nanocarbons. *Small* **2016**, *12*, 5684-5691.

(118) He, T.; Su, Q.; Yildiz, Z.; Cai, K.; Wang, Y. Ultrafine Carbon Fibers with Hollow-Porous Multilayered Structure for Supercapacitors. *Electrochimica Acta* **2016**, *222*, 1120-1127.

(119) Li, Y.; Li, Z.; Shen, P. K. Simultaneous formation of ultrahigh surface area and three-dimensional hierarchical porous graphene-like networks for fast and highly stable supercapacitors. *Adv Mater* **2013**, *25*, 2474-2480.

(120) Ruiz, V.; Pandolfo, A. High-frequency carbon supercapacitors from polyfurfuryl alcohol. *Journal of Power Sources* **2011**, *196*, 7816-7822.

(121) Gao, F.; Wolfer, M. T.; Nebel, C. E. Highly porous diamond foam as a thin-film micro-supercapacitor material. *Carbon* **2014**, *80*, 833-840.

(122) Thissandier, F.; Gentile, P.; Brousse, T.; Bidan, G.; Sadki, S. Are tomorrow's micro-supercapacitors hidden in a forest of silicon nanotrees? *Journal of Power Sources* **2014**, *269*, 740-746.

(123) Pan, X.; Ren, G.; Hoque, M. N. F.; Bayne, S.; Zhu, K.; Fan, Z. Fast Supercapacitors Based on Graphene- Bridged V2O3/VOx Core–Shell Nanostructure Electrodes with a Power Density of 1 MW kg− 1. *Advanced Materials Interfaces* **2014**, *1*, 1400398.

(124) Yang, P.; Chao, D.; Zhu, C.; Xia, X.; Zhang, Y.; Wang, X.; Sun, P.; Tay, B. K.; Shen, Z. X.; Mai, W. Ultrafast- Charging Supercapacitors Based on Corn- Like Titanium Nitride Nanostructures. *Advanced Science* **2015**, *3*, 1500299.

(125) Liu, W.; Lu, C.; Wang, X.; Tay, R. Y.; Tay, B. K. High-performance microsupercapacitors based on two-dimensional graphene/manganese dioxide/silver nanowire ternary hybrid film. *ACS nano* **2015**, *9*, 1528-1542.

(126) Shen, B.; Lang, J.; Guo, R.; Zhang, X.; Yan, X. Engineering the Electrochemical Capacitive Properties of Microsupercapacitors Based on Graphene Quantum Dots/MnO2 Using Ionic Liquid Gel Electrolytes. *ACS applied materials & interfaces* **2015**, *7*, 25378-25389.

(127) Kurra, N.; Jiang, Q.; Syed, A.; Xia, C.; Alshareef, H. N. Micro-Pseudocapacitors with Electroactive Polymer Electrodes: Toward AC-Line Filtering Applications. *ACS applied materials & interfaces* **2016**, *8*, 12748-12755.

(128) Yu, G.; Xie, X.; Pan, L.; Bao, Z.; Cui, Y. Hybrid nanostructured materials for high-performance electrochemical capacitors. *Nano Energy* **2013**, *2*, 213-234.

(129) Peng, L.; Zhu, Y.; Li, H.; Yu, G. Chemically Integrated Inorganic-Graphene Two-Dimensional Hybrid Materials for Flexible Energy Storage Devices. *Small* **2016**, *12*, 6183-6199.

(130) Bonaccorso, F.; Colombo, L.; Yu, G.; Stoller, M.; Tozzini, V.; Ferrari, A. C.; Ruoff, R. S.; Pellegrini, V. 2D materials. Graphene, related two-dimensional crystals, and hybrid systems for energy conversion and storage. *Science* **2015**, *347*, 1246501.

(131) Pan, X.; Zhao, Y.; Ren, G.; Fan, Z. Highly conductive VO 2 treated with hydrogen for supercapacitors. *Chemical Communications* **2013**, *49*, 3943-3945.

(132) Lu, X.; Wang, G.; Zhai, T.; Yu, M.; Xie, S.; Ling, Y.; Liang, C.; Tong, Y.; Li, Y. Stabilized TiN nanowire arrays for high-performance and flexible supercapacitors. *Nano letters* **2012**, *12*, 5376-5381.

(133) Peng, L.; Zhu, Y.; Chen, D.; Ruoff, R. S.; Yu, G. Two-Dimensional Materials for Beyond-Lithium-Ion Batteries. *Advanced Energy Materials* **2016**, *6*, 1600025-n/a.

(134) Feng, J.; Sun, X.; Wu, C.; Peng, L.; Lin, C.; Hu, S.; Yang, J.; Xie, Y. Metallic Few-Layered VS2 Ultrathin Nanosheets: High Two-Dimensional Conductivity for In-Plane Supercapacitors. *Journal of the American Chemical Society* **2011**, *133*, 17832-17838.

(135) Acerce, M.; Voiry, D.; Chhowalla, M. Metallic 1T phase MoS2 nanosheets as supercapacitor electrode materials. *Nat Nanotechnol* **2015**, *10*, 313-318.

(136) Khalil, A.; Liu, Q.; He, Q.; Xiang, T.; Liu, D.; Wang, C.; Fang, Q.; Song, L. Metallic 1T-WS2 nanoribbons as highly conductive electrodes for supercapacitors. *RSC Advances* **2016**, *6*, 48788-48791.

(137) Bissett, M. A.; Worrall, S. D.; Kinloch, I. A.; Dryfe, R. A. W. Comparison of Two-Dimensional Transition Metal Dichalcogenides for Electrochemical Supercapacitors. *Electrochimica Acta* **2016**, *201*, 30-37.

(138) Kurra, N.; Hota, M. K.; Alshareef, H. N. Conducting polymer micro-supercapacitors for flexible energy storage and AC line-filtering. *Nano Energy* **2015**, *13*, 500-508.

(139) Li, Z.; Ma, G.; Ge, R.; Qin, F.; Dong, X.; Meng, W.; Liu, T.; Tong, J.; Jiang, F.; Zhou, Y. Free- Standing Conducting Polymer Films for High- Performance Energy Devices. *Angewandte Chemie* **2016**, *128*, 991-994.

(140) Wu, H.; Wang, X.; Jiang, L.; Wu, C.; Zhao, Q.; Liu, X.; Yi, L. The effects of electrolyte on the supercapacitive performance of activated calcium carbide-derived carbon. *Journal of Power Sources* **2013**, *226*, 202-209.

(141) Wang, Y.; Zheng, C.; Qi, L.; Yoshio, M.; Yoshizuka, K.; Wang, H. Utilization of (oxalato) borate-based organic electrolytes in activated carbon/graphite capacitors. *Journal of Power Sources* **2011**, *196*, 10507-10510.

(142) Galiński, M.; Lewandowski, A.; Stępniak, I. Ionic liquids as electrolytes. *Electrochimica Acta* **2006**, *51*, 5567-5580.

(143) Arbizzani, C.; Biso, M.; Cericola, D.; Lazzari, M.; Soavi, F.; Mastragostino, M. Safe, high-energy supercapacitors based on solvent-free ionic liquid electrolytes. *Journal of Power Sources* **2008**, *185*, 1575-1579.

(144) Mousavi, M. P.; Wilson, B. E.; Kashefolgheta, S.; Anderson, E. L.; He, S.; Bühlmann, P.; Stein, A. Ionic Liquids as Electrolytes for Electrochemical Double-Layer Capacitors: Structures that Optimize Specific Energy. *ACS applied materials & interfaces* **2016**, *8*, 3396-3406.

(145) De Vos, N.; Maton, C.; Stevens, C. V. Electrochemical stability of ionic liquids: general influences and degradation mechanisms. *ChemElectroChem* **2014**, *1*, 1258-1270.

(146) Chmiola, J.; Largeot, C.; Taberna, P.-L.; Simon, P.; Gogotsi, Y. Monolithic carbide-derived carbon films for micro-supercapacitors. *Science* **2010**, *328*, 480-483.

(147) Kyerematen, N. A.; Brousse, T.; Pech, D. Microsupercapacitors as miniaturized energy-storage components for on-chip electronics. *Nature Nanotechnology* **2017**, *12*, 7-15.

(148) Huang, P.; Lethien, C.; Pinaud, S.; Brousse, K.; Laloo, R.; Turq, V.; Respaud, M.; Demortiere, A.; Daffos, B.; Taberna, P. L.; Chaudret, B.; Gogotsi, Y.; Simon, P. On-chip and freestanding elastic carbon films for micro-supercapacitors. *Science* **2016**, *351*, 691-695.

(149) Wu, Z.-S.; Feng, X.; Cheng, H.-M. Recent advances in graphene-based planar micro-supercapacitors for on-chip energy storage. *National Science Review* **2014**, *1*, 277-292.

(150) Beidaghi, M.; Gogotsi, Y. Capacitive energy storage in micro-scale devices: recent advances in design and fabrication of micro-supercapacitors. *Energy & Environmental Science* **2014**, *7*, 867-884.

(151) Durou, H.; Pech, D.; Colin, D.; Simon, P.; Taberna, P.-L.; Brunet, M. Wafer-level fabrication process for fully encapsulated micro-supercapacitors with high specific energy. *Microsystem technologies* **2012**, *18*, 467-473.

(152) Liu, Z.; Wu, Z. S.; Yang, S.; Dong, R.; Feng, X.; Müllen, K. Ultraflexible In- Plane Micro- Supercapacitors by Direct Printing of Solution- Processable Electrochemically Exfoliated Graphene. *Adv Mater* **2016**, *28*, 2217-2222.

(153) El-Kady, M. F.; Strong, V.; Dubin, S.; Kaner, R. B. Laser scribing of high-performance and flexible graphene-based electrochemical capacitors. *Science* **2012**, *335*, 1326-1330.

(154) Lin, J.; Peng, Z.; Liu, Y.; Ruiz-Zepeda, F.; Ye, R.; Samuel, E. L.; Yacaman, M. J.; Yakobson, B. I.; Tour, J. M. Laser-induced porous graphene films from commercial polymers. *Nature communications* **2014**, *5*, 5714.

(155) In, J. B.; Hsia, B.; Yoo, J.-H.; Hyun, S.; Carraro, C.; Maboudian, R.; Grigoropoulos, C. P. Facile fabrication of flexible all solid-state micro-supercapacitor by direct laser writing of porous carbon in polyimide. *Carbon* **2015**, *83*, 144-151.

(156) Gao, W.; Singh, N.; Song, L.; Liu, Z.; Reddy, A. L.; Ci, L.; Vajtai, R.; Zhang, Q.; Wei, B.; Ajayan, P. M. Direct laser writing of micro-supercapacitors on hydrated graphite oxide films. *Nat Nanotechnol* **2011**, *6*, 496-500.

(157) Lang, X.; Hirata, A.; Fujita, T.; Chen, M. Nanoporous metal/oxide hybrid electrodes for electrochemical supercapacitors. *Nature Nanotechnology* **2011**, *6*, 232-236.

(158) Han, J.; Lin, Y. C.; Chen, L.; Tsai, Y. C.; Ito, Y.; Guo, X.; Hirata, A.; Fujita, T.; Esashi, M.; Gessner, T. On- Chip Micro- Pseudocapacitors for Ultrahigh Energy and Power Delivery. *Advanced Science* **2015**, *2*, 1500067.

(159) Wu, Z. S.; Parvez, K.; Li, S.; Yang, S.; Liu, Z.; Liu, S.; Feng, X.; Müllen, K. Alternating Stacked Graphene- Conducting Polymer Compact Films with Ultrahigh Areal and Volumetric Capacitances for High- Energy Micro- Supercapacitors. *Adv Mater* **2015**, *27*, 4054-4061.

(160) Laszczyk, K. U.; Kobashi, K.; Sakurai, S.; Sekiguchi, A.; Futaba, D. N.; Yamada, T.; Hata, K. Lithographically Integrated Microsupercapacitors for Compact, High Performance, and Designable Energy Circuits. *Advanced Energy Materials* **2015**, *5*, 1500741.

(161) Luryi, S. Quantum capacitance devices. *Applied Physics Letters* **1988**, *52*, 501-503.

(162) Xia, J.; Chen, F.; Li, J.; Tao, N. Measurement of the quantum capacitance of graphene. *Nat Nanotechnol* **2009**, *4*, 505-509.

(163) Zhou, S.; Gweon, G.-H.; Graf, J.; Fedorov, A.; Spataru, C.; Diehl, R.; Kopelevich, Y.; Lee, D.-H.; Louie, S. G.; Lanzara, A. First direct observation of Dirac fermions in graphite. *Nature physics* **2006**, *2*, 595-599.

(164) Randin, J.-P.; Yeager, E. Differential capacitance study of stress-annealed pyrolytic graphite electrodes. **1971**, *118*, 711-714.

(165) Randin, J.-P.; Yeager, E. Differential capacitance study on the basal plane of stress-annealed pyrolytic graphite. *Journal of Electroanalytical Chemistry and Interfacial Electrochemistry* **1972**, *36*, 257-276.

(166) Kurzweil, P.: Electrochemical double-layer capacitors. In *Encyclopedia of electrochemical power sources*; Garche, J., Ed.; Elsevier, 2009.

(167) Vatamanu, J.; Ni, X.; Liu, F.; Bedrov, D. Tailoring graphene-based electrodes from semiconducting to metallic to increase the energy density in supercapacitors. *Nanotechnology* **2015**, *26*, 464001.

(168) Kim, S.-K.; Kim, H. J.; Lee, J.-C.; Braun, P. V.; Park, H. S. Extremely durable, flexible supercapacitors with greatly improved performance at high temperatures. *ACS nano* **2015**, *9*, 8569-8577.

Dr. Zhaoyang Fan Obtained his B.E and M.E degrees from Tsinghua University of China and Ph.D. from Northwestern University of U.S. He is an associate professor in Department of Electrical and Computer Engineering and Nano Tech Center, Texas Tech University. His research concerns synthesis and property study of nanomaterials and semiconductors, and their applications for photonics and clean energy.

Ms. Nazifah Islam is a Ph.D. student in the Department of Electrical and Computer Engineering at Texas Tech University under supervision of Prof. Zhaoyang Fan. She completed her Bachelor degree from Bangladesh University of Engineering and Technology. Her research interest includes studies of nanostructured materials for energy conversion and storage devices. She is currently working on development of electrode material and design towards compact high-frequency supercapacitors.

Dr. Stephen B. Bayne received his PhD, MS and BS degrees in Electrical Engineering from Texas Tech University. After completing his Doctoral studies, he joined the Naval Research Lab (NRL) where he was an electronics engineer designing advanced power electronics systems for space power applications. After two and a half years at NRL, Dr. Bayne transferred to the Army Research Lab (ARL) where he was instrumental in developing a high temperature power electronic program. Dr. Bayne transitioned over to academia where he is a Professor at Texas Tech University. His research interests are Power Electronics, Pulse Power and Renewable Energy.